Research Square

Preprints are preliminary reports that have not undergone peer review.
They should not be considered conclusive, used to inform clinical practice,
or referenced by the media as validated information.

Emerging Heat Wave Hotspots in Sri Lanka: The Role of Ocean–Atmosphere Coupling

Prabashvari Galagamage
University of Ruhuna
Gayan Pathirana
upgpathirana@fish.ruh.ac.lk
University of Ruhuna https://orcid.org/0000-0002-4670-579X
Xin Geng
Nanjing University of Information Science and Technology
Dongxiao Wang
Sun Yat-Sen University
Upul Premarthne
University of Ruhuna

Research Article

Keywords: Heat waves, Sri Lanka, Monsoon variability, Indian Ocean warming, Ocean–atmosphere coupling, Tropical climate extremes

Posted Date: August 31st, 2026

DOI: https://doi.org/10.21203/rs.3.rs-10697012/v1

License: This work is licensed under a Creative Commons Attribution 4.0 International License.
Read Full License

Emerging Heat Wave Hotspots in Sri Lanka: The Role of Ocean–Atmosphere Coupling

Prabashvari Galagamage[1], Gayan Pathirana[1,2*], Xin Geng[3], Dongxiao Wang[4*], Upul Premarthne[1]

[1]Department of Oceanography and Marine Geology, Faculty of Fisheries and Marine Sciences & Technology, University of Ruhuna, Matara, Sri Lanka.

[2]Center for Climate Change Studies, Matara, Sri Lanka.

[3]Nanjing University of Information Science & Technology, China.

[4]School of Marine Science, Sun Yat-sen University: Southern Marine Science and Engineering Guangdong Laboratory, Zhuhai, China.

[*]Correspondence to:

Dr. Gayan Pathirana (Email: upgpathirana@fish.ruh.ac.lk, Phone: +94717439611)

ORCID: https://orcid.org/0000-0002-4670-579X

Address: Department of Oceanography and Marine Geology, Faculty of Fisheries and Marine Sciences & Technology, University of Ruhuna, Matara, Sri Lanka.

Professor Dongxiao Wang (Email: dxwang@mail.sysu.edu.cn)

Address: School of Marine Science, Sun Yat-sen University: Southern Marine Science and Engineering Guangdong Laboratory, Zhuhai, China.

Abstract

Heat waves (HWs) are emerging as a major climate hazard across tropical regions, yet their climatological characteristics and governing physical mechanisms remain poorly understood in Sri Lanka. This study presents the first comprehensive assessment of seasonal HW variability and associated ocean–atmosphere drivers over Sri Lanka using ERA5 reanalysis data for the period 1995–2024. HWs were identified using a percentile-based threshold applied to daily maximum temperature (T_{max}), and their frequency, duration, and intensity were examined across the four monsoonal seasons. The results reveal pronounced spatial and seasonal contrasts in HW behaviour across the island. The First Inter-Monsoon (FIM) season exhibits the strongest HW regime, characterized by the highest proportional occurrence of HW days, elevated intensities, and long event duration under conditions of strong solar heating and weak atmospheric ventilation. In contrast, during the Southwest Monsoon (SWM), HW activity becomes concentrated over the eastern and southeastern dry-zone lowlands as the central highlands generate a pronounced rain-shadow effect that suppresses cloud formation and rainfall on the leeward side of the island. Composite analyses show that HW days are consistently associated with enhanced large-scale subsidence linked to variability in the Walker and Hadley circulations, leading to suppressed convection, reduced cloud cover, and positive Outgoing Longwave Radiation (OLR) anomalies across the northern Indian Ocean. These conditions promote enhanced surface shortwave radiation and radiative amplification of near-surface temperatures. Concurrent rainfall deficits and reduced boundary-layer humidity further intensify and sustain heat extremes through land–atmosphere feedback processes. In addition, HW conditions indicating enhanced evaporative stress and reduced latent cooling. In addition, HW conditions occur alongside positive Sea Surface Temperature (SST) anomalies across the tropical Indian Ocean, indicating that Sri Lankan HWs are embedded within a broader basin-scale warm ocean–atmosphere state that reinforces atmospheric stability and persistent hot conditions. Together, these findings demonstrate that HWs in Sri Lanka arise from tightly coupled ocean–atmosphere–land interactions rather than from local temperature anomalies alone. The identification of distinct seasonal HW regimes and persistent regional hotspots provides an important scientific basis for improving climate-risk assessment and adaptation planning in the rapidly warming Indian Ocean region.

Keywords: Heat waves; Sri Lanka; Monsoon variability; Indian Ocean warming; Ocean–atmosphere coupling; Tropical climate extremes

1 Introduction

Heat Waves (HWs) are prolonged periods of anomalously high near-surface air temperature relative to the local climatological baseline, typically persisting for several consecutive days (Perkins & Alexander, 2013). Unlike short-lived temperature extremes, HWs represent sustained thermal stress events whose impacts accumulate over time, affecting human health, agriculture, ecosystems, and energy systems (Perkins, 2015; Horton et al., 2016; IPCC, 2023b; Wu et al., 2023; WHO, 2024). Their severity is further amplified in humid environments, where reduced evaporative cooling enhances physiological heat stress (Cvijanovic et al., 2023). The increasing scientific and societal focus on HWs reflects their emergence as the deadliest major global hazard (Barriopedro et al., 2023). Extreme heat events have been linked to increased mortality (Miralles et al., 2014), agricultural losses, ecosystem stress, reduced labour productivity, and increased energy demand across both developed and developing regions (Horton et al., 2016). Despite their global significance, there is no universally accepted definition of HWs, largely due to regional differences in climate variability and impact thresholds (Robinson, 2001; Perkins & Alexander, 2013). Consequently, percentile-based approaches, where temperature extremes are defined relative to local climatology, have become widely adopted, particularly for comparative analyses across diverse climatic regimes (Alexander et al., 2006; Perkins & Alexander, 2013; Perkins, 2015; Sharma et al., 2022; Cvijanovic et al., 2023).

The increasing frequency and intensity of HWs represent one of the most robust signals of climate change (IPCC, 2023a). Observations indicate widespread increases in the frequency, duration, and intensity of extreme temperature events across most land regions since the mid-twentieth century (Seneviratne et al., 2021). Beyond thermodynamic warming, these changes are strongly modulated by dynamical processes within the climate system, including atmospheric circulation variability, land–atmosphere feedbacks, cloud–radiation interactions, and ocean–atmosphere coupling (Seneviratne et al., 2010; Horton et al., 2016). In particular, persistent HWs are commonly associated with large-scale subsidence, suppressed convection, and reduced cloud cover, which enhance incoming shortwave radiation and promote surface warming (Trenberth & Fasullo, 2012; Barriopedro et al., 2023).

While HW dynamics are well documented in mid-latitude regions, their governing mechanisms in the tropics remain less clearly understood. In contrast to mid-latitude blocking systems, tropical

HWs are more strongly influenced by variations in convection, vertical motion, cloud cover, and radiative fluxes (Horton et al., 2016; Perkins-Kirkpatrick & Lewis, 2020). High background humidity further intensifies heat stress, even under moderate temperature anomalies, highlighting the importance of moisture–temperature coupling in these regions (Sherwood & Huber, 2010). These distinct characteristics underscore the need for region-specific, process-based assessments of HW behaviour in tropical climates.

The Indian Ocean plays a critical role in modulating regional climate variability across South Asia through its strong influence on atmospheric circulation, convection, and rainfall (Roxy et al., 2014; Cai et al., 2014, 2015, 2018; Pathirana et al., 2023). Rapid warming of the tropical Indian Ocean has altered large-scale circulation patterns, including the Walker and Hadley circulations, with implications for cloud formation, subsidence, and surface energy balance (Roxy et al., 2015; Xie et al., 2016). Variations in Sea Surface Temperature (SST) gradients can therefore influence the occurrence and persistence of heat extremes by modulating atmospheric stability and radiative fluxes. However, the role of these coupled ocean–atmosphere processes in shaping HW characteristics over tropical island environments remains poorly understood. This gap is particularly relevant for tropical islands such as Sri Lanka, where ocean-atmosphere interactions strongly influence local climate variability.

While large-scale atmospheric and oceanic drivers provide the necessary conditions for HW occurrence, local land-atmosphere feedback processes, particularly soil moisture-temperature coupling, act as critical intensifiers (Ford & Schoof, 2017; Miralles et al., 2012). Soil moisture controls the energy budget by partitioning net radiation between latent and sensible heat fluxes (Yuan et al., 2019). Surface moisture depletion during HW reduces evaporative cooling (latent heat) (Benson & Dirmeyer, 2021). It leads to a rapid increase in near-surface temperatures (sensible heat), further desiccating the soil in a positive feedback loop (Liu & Pu, 2019). Understanding this feedback is essential for characterizing the persistence of a regional hotspot in a tropical island setting.

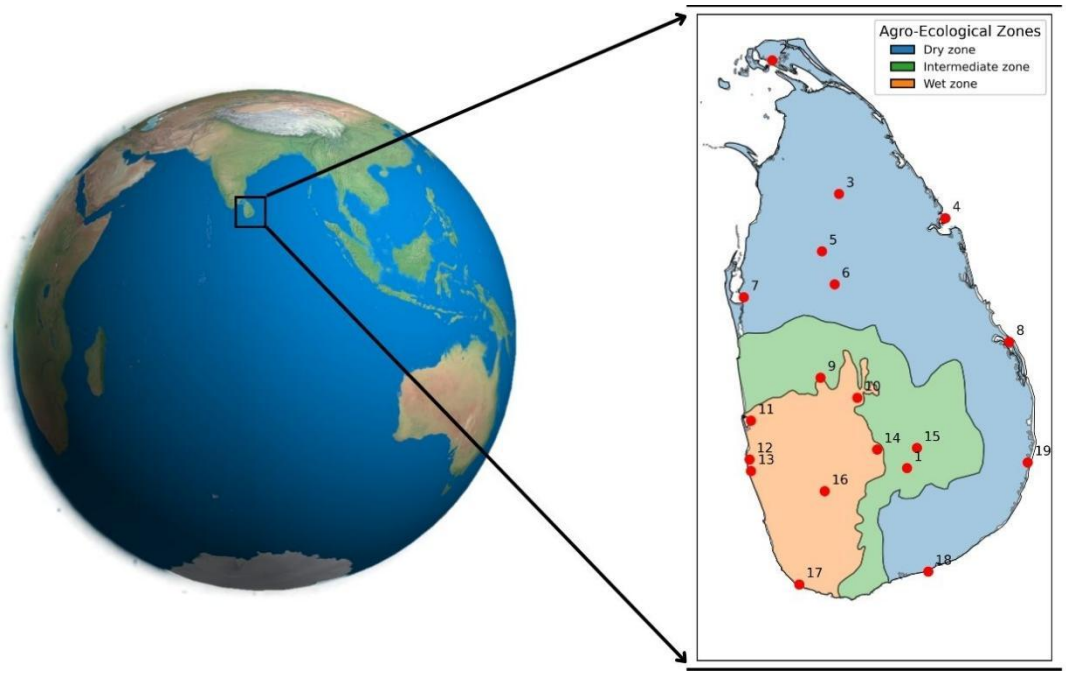


Fig. 1 Geographical Location and Agro-ecological Climatic Zone (Dry-Zone: annual rainfall < 1750 mm, Intermediate-Zone: annual rainfall 1750 – 2500 mm, and Wet-Zone: annual rainfall > 2500 mm) of Sri Lanka. Red dots indicate the locations of the 19 meteorological observation stations used in this study. The Inset globe shows Sri Lanka's geographic position within the broader Indian Ocean region. (Details of the station network are provided in Table S1).

Sri Lanka, located at the southern tip of the Indian subcontinent (5°55'- 9°51' N and 79°42'- 81°53' E; Fig. 1), provides a unique setting to investigate these processes. The island's climate is strongly governed by monsoon circulation and exhibits pronounced seasonal variability associated with the Northeast Monsoon (NEM, December–February), First Inter-Monsoon (FIM, March–April), Southwest Monsoon (SWM, May–September), and Second Inter-Monsoon (SIM, October–November) (Karunathilaka et al., 2017; Punyawardena et al., 2020; Abeysekera et al., 2021). These seasonal regimes modulate cloud cover, rainfall, wind patterns, and humidity (Suppiah & Yoshino, 1984; Suppiah, 1996), thereby influencing surface energy balance and the persistence of high-temperature anomalies. In addition, marked spatial heterogeneity, characterized by wet, intermediate, and dry climatic zones, creates distinct regional environments with varying susceptibility to heat extremes.

Despite its climate complexity and vulnerability, systematic assessments of HWs in Sri Lanka remain limited. Previous studies have primarily focused on precipitation variability, with relatively few investigations addressing temperature extremes using high-resolution daily data (Jayawardena et al., 2018; Keshav et al., 2026). Moreover, existing analyses have largely emphasized statistical characterization, with limited attention to the underlying physical drivers. As a result, key uncertainties persist regarding the spatial distribution, seasonal variability, and governing mechanisms of HWs across the island. In particular, the role of ocean-atmosphere coupling, circulation variability, and surface energy balance processes in modulating HW development and persistence remains insufficiently understood. While the ERA5 reanalysis product is widely used for temperature extreme studies, its 0.25° (~28 km) spatial resolution warrants careful validation in regions of complex topography such as Sri Lanka, where mesoscale temperature gradients associated with the central highlands may not be fully resolved. To strengthen confidence in the identified HW hotspots, the present study therefore includes a rigorous point-to-pixel comparison of ERA5 daily maximum temperature (T_{max}) against independent station observations. In this context, the present study provides a comprehensive, process-oriented assessment of HWs characteristics in Sri Lanka. Using gridded temperature data for the period 1995–2024, this study quantifies the frequency, intensity, and duration of HWs and identifies emerging hotspot regions across different climatic zones. Furthermore, it investigates the seasonal variability of HWs within the monsoon framework and examines the role of ocean–atmosphere coupling in modulating their development and persistence through analyses of key atmospheric and oceanic variables. By linking large-scale climate processes to regional heat extremes, this study provides new insights into the drivers of HWs in a tropical island setting and offers a foundation for improved climate risk assessment and adaptation strategies in Sri Lanka.

2 Data and Methodology

2.1 Data

T_{max} was obtained from the ERA5 reanalysis produced by the European Centre for Medium-Range Weather Forecasts (ECMWF; Hersbach et al., 2020). ERA5 provides globally consistent atmospheric variables with high spatial and temporal resolution and has been widely used in studies of climate variability and temperature extremes. T_{max} was obtained from the 2-m air

temperature (t2m) variable for the period 1995-2024. The gridded dataset (0.25° × 0.25°) was spatially constrained to the land area of Sri Lanka using a national boundary shape file to exclude surrounding ocean grid cells.

To investigate the large-scale drivers of HW variability, additional atmospheric and oceanic variables were analyzed over the Indian Ocean region. SST data were obtained from the NOAA Optimum Interpolation Sea Surface Temperature (OISST) Version 2.1 dataset, which provides daily global SST fields at 0.25° spatial resolution based on combined satellite and in-situ observations (Reynolds et al., 2007). Outgoing Longwave Radiation (OLR) was obtained from the NOAA Daily OLR Climate Data Record, which provides satellite-derived estimates of top-of-atmosphere long-wave radiation at 1° spatial resolution (Lee, 2014). Vertical motion was examined at 500 hPa, representing mid-tropospheric subsidence and ascent at 0.25° spatial resolution. To characterize large-scale circulation structure, including the Hadley and Walker cells, vertical velocity fields across multiple pressure levels (1000-100 hPa) were also analyzed. Surface wind fields were derived from the 10-m zonal (u10) and meridional (v10) wind components, representing the horizontal wind velocity at 10m above the surface at 0.25° spatial resolution for the study period. Daily total precipitation (mm/day) at 0.25° spatial resolution was analyzed to examine anomalous rainfall during the study period and to investigate the suppression of convective rainfall activity. Shortwave Radiation represents the total amount of solar radiation, derived from the downwelling shortwave flux at 0.25° spatial resolution. Low cloud cover (LCC) and high cloud cover (HCC) at 0.25° spatial resolution were analyzed to characterize cloud variability relevant to radiative and convective. Vertical velocity, Surface wind fields, Daily total precipitation, Shortwave, LCC and HCC were obtained from ERA5 reanalysis datasets produced by the ECMWF (Hersbach et al., 2020). Near-surface relative humidity (RH, %) was obtained from the AgERA5 dataset (Boogaard et al., 2020), which provides daily agro-meteorological variables at 0.25° spatial resolution derived from ERA5 with bias-correlations and tailored processing designed for surface-layer and agricultural applications. Daily surface volumetric soil moisture was obtained from the C3S Satellite Surface Soil Moisture merged combined product. This dataset integrates active and passive microwave remote sensing observations at a 0.25° spatial resolution (Dorigo et al., 2017).

To assess the reliability of ERA5 T_{max} for HW analysis, daily T_{max} observations from 19 meteorological stations (Table S1) were obtained from the Department of Meteorology Sri Lanka, under a university-approved research grant for the period 1995-2024 and used as an independent reference dataset.

All variables were analyzed at daily temporal resolution over the period 1995-2024 and were subsequently classified according to the four climatological seasons of Sri Lanka. Table S2 in the supplementary material summarizes the dataset used in this study. Data processing, statistical calculations, and visualization were carried out using the Python programming language with supportive libraries.

2.2 Methodology

2.2.1 Seasonal Classification

All analyses were conducted within the framework of the four climatological seasons that represent the Sri Lankan monsoon cycle: NEM, FIM, SWM, and SIM (Karunathilaka et al., 2017; Punyawardena et al., 2020). This seasonal classification reflects the distinct rainfall regimes and large-scale atmospheric circulation patterns that govern Sri Lanka's climate, which differ substantially from standard astronomical seasons used in extra-tropical studies. For consistency, December was assigned to the following year to preserve the complete December-February seasonal cycle.

2.2.2 Seasonal Climatology and Variability of Maximum Temperature

Seasonal climatological mean T_{max} fields were computed by averaging T_{max} across all years (1995-2024) for each season. Seasonal variability of T_{max} was quantified using the standard deviation (STD) of daily T_{max} at each grid point. For visualization purposes, the gridded temperature fields were interpolated to a higher-resolution grid using a nearest-neighbour interpolation approach. A land mask based on the Sri Lankan boundary shape file was applied to retain only terrestrial grid points.

2.2.3 Long-term Trends in T_{max}

Long-term changes in T_{max} were assessed by estimating linear trends in seasonal mean temperature over the study period. Daily T_{max} values were first aggregated into seasonal means for each year, and trends were then calculated using ordinary least squares regression (Wilks, 2011). Trend magnitudes are expressed in degrees Celsius per decade (°C/decade). The statistical significance of the trends was assessed using the p-value associated with the regression slope, with significance defined at the 95% confidence level ($p < 0.05$).

2.2.4 Heat Wave Identification

HWs were identified at each grid point using a percentile-based relative threshold approach, which accounts for local climatological variability and is particularly suitable for tropical regions (Perkins and Alexander, 2013; Perkins-Kirkpatrick and Lewis, 2020). For each calendar day, a threshold was defined as the 95th percentile of T_{max} computed using a ±15-day moving window centred on that day. Day-of-year were calculated on a 366-day calendar to account for leap years, with the percentile threshold window (±15 days) wrapping around the year boundary to ensure adequate sample sizes for 29th of February. When normalizing HW frequency by the total number of events per season, leap years were accounted for by using the actual calendar days for each year, ensuring accurate percentage calculations across the 1995-2024 study period. This produced a seasonally varying threshold that capture the annual cycle. A HW event was defined as a period of at least three consecutive days during which T_{max} exceeded the corresponding threshold (Collins et al., 2000; Perkins and Alexander, 2013; Russo et al., 2015). To avoid artificial fragmentation of events, a 4-day separation rule was applied, whereby exceedance periods separated by fewer than four days were treated as part of the same event (Fischer & Schär, 2010; Perkins & Alexander, 2013).

To assess the robustness of hotspot identification, the primary 95th percentile threshold was compared with an alternative 90th percentile threshold. The resulting seasonal HW frequency maps were examined to determine whether the major HW hotspot regions remained consistent across the threshold choices.

2.2.5 Spatial Aggregation and Event Characterization

Grid-point HW occurrences were aggregated spatially and temporally to derive island-wide metrics and event-based characteristics across the seasons. At each grid point, the following metrics were computed to describe the spatial distribution of HW properties: frequency (total number of HW events), mean intensity (mean T_{max} during HW days), maximum intensity (peak T_{max} during recorded HW events), minimum intensity (weakest T_{max} during recorded HW events), mean duration (mean length of all events in days at each grid points), and strongest duration (length of the longest recorded event). The strongest-duration metric is the longest individual HW event recorded at each grid point across the study period. Therefore, it provides insight into the maximum persistence of HW conditions across Sri Lanka. Seasonal HW contribution was calculated as the ratio of the number of events occurring within each season to the total number of days in that season, expressed as a percentage. This normalization is essential for meaningful cross-seasonal comparisons, as raw frequency counts would systematically favour the longer SWM season independent of any genuine difference in HW propensity (Perkins & Alexander, 2013; Russo et al., 2015; Perkins-Kirkpatrick & Lewis, 2020). These metrics collectively provide a comprehensive characterization of the spatial heterogeneity of the HW hazard across Sri Lanka.

To identify larger-scale events, grid-level occurrences were temporally merged and filtered based on spatial extent. An event was classified as a major HW only when it affected at least 80 grid cells simultaneously, corresponding to approximately 20% of the total terrestrial domain. This spatial extent threshold was adopted to ensure that retained events represented coherent, climatically meaningful episodes driven by large-scale atmospheric forcing, rather than isolated local exceedance arising from meso-scale or topographically forced temperature anomalies.

2.2.6 Heat Wave Metrics Trend Analysis

This study quantifies long-term changes in HW characteristics using HW frequency, maximum intensity, and strongest duration. To assess long-term trends, annual seasonal time series of each metric were analyzed using ordinary least square (OLS) regression. The regression slope represents the rate of change per year. Statistical significance was evaluated at the 95% confidence level ($p < 0.05$), and the coefficient of determination (R^2) was used to assess the explanatory power of the linear trend relative to interannual variability.

2.2.7 Composite Analyses

To diagnose the environmental conditions associated with HW development, composite analyses were performed separately for HW and non-heat wave (non-HW) days for each season. Variables included in the composite analyses were SST, 10-m surface winds, vertical velocity, precipitation, OLR, Shortwave Radiation, near-surface RH, LCC, HCC, and Surface Soil Moisture. Before composite calculation, daily anomalies for each variable were computed by subtracting the seasonal climatological mean from the raw daily values, thereby isolating sub-seasonal variability from the annual cycle. Composite mean anomalies were computed separately for HW and non-HW days, and composite differences (HW – non-HW) were calculated to isolate the thermodynamic, radiative, and dynamical conditions specifically associated with HW occurrence relative to typical seasonal conditions. This approach effectively suppresses the influence of the seasonal cycle and long-term trend on the composite signal, ensuring that identified anomalies reflect synoptic-to-intra-seasonal forcing rather than climatological mean differences between seasons (Wu et al., 2023). The composite framework facilitates identification of compound hot-dry conditions linked to land-atmosphere feedbacks, consistent with recent studies demonstrating the role of precipitation deficits and reduced soil moisture in amplifying surface heat extremes (Hassan et al., 2024).

2.2.8 Statistical Significance

The statistical significance of composite differences between HW and non-HW conditions was assessed using a two-sided Welch's t-test (Wilks, 2011), which does not assume equal variances between the samples. Composite differences were considered statistically significant at the 95% confidence level ($p < 0.05$). This significance framework was applied to the circulation, thermodynamic, and surface driver composites.

2.2.9 Validation of ERA5 T_{max} against Station Observations

To evaluate the reliability of ERA5 T_{max} over a region of complex topography, a point-to-pixel comparison was performed between ERA5 and the 19 meteorological station records described in

section 2.1. For each station, daily ERA5 T_{max} was extracted from the nearest 0.25° grid cell to the station coordinates, and the resulting paired time series were compared over their common overlapping period. Agreement between ERA5 and the observations was quantified using three complementary metrics: the Pearson correlation coefficient (r), which assesses the temporal agreement between the two records; the Mean Bias (MB), which identifies systematic over-or under-estimation; and the Root Mean Square Error (RMSE), which quantifies the overall magnitude of absolute error.

2.2.10 Abbreviations

CDS	Climate Data Store
ECMWF	European Center for Medium-range Weather Forecasts Reanalysis
ENSO	El Niño Southern Oscillation
FIM	First Inter-monsoon
HCC	High Cloud Cover
HW	Heat wave
IOBM	Indian Ocean Basin Mode
IOD	Indian Ocean Dipole
LCC	Low Cloud Cover
MB	Mean Bias
NEM	North East Monsoon

Non-HW	Non-Heat Wave
OISST	Optimum Interpolation Sea Surface Temperature
OLR	Outgoing Longwave Radiation
OLS	Ordinary Least Squares
RH	Relative Humidity
RMSE	Root Mean Square Error
SIM	Second Inter-monsoon
SST	Sea Surface Temperature
STD	Standard Deviation
SWM	Southwest Monsoon
T_{max}	Daily Maximum near-surface air Temperature

3 Results

3.1 Validation Result of ERA5 T_{max} against Station Observations

The point-to-pixel comparison between ERA5 T_{max} 19 observational stations (Fig. 2; Fig. S1) demonstrates an overall high level of agreement across Sri Lanka. The strongest temporal agreement was observed at Trincomalee (r = 0.92) and Vavuniya (r = 0.91), both located within the dry-zone HW hotspot regions identified in sections 3.4 and 3.5. Correlation remains

consistently high (r > 0.8) across the majority of dry-zone and lowlands stations, indicating that ERA5 reproduces the day-to-day evolution of T_{max} with high fidelity in these areas.

Bias and error metrics reveal a clear elevation dependence (Fig. 2b), consistent with the topographic concern raised regarding ERA5's 0.25° resolution. High-elevation stations such as Nuwara Eliya (1880 m) show a pronounced warm bias (+3.49 °C), while low-lying coastal stations such as Jaffna show a cold bias (-2.92 °C). RMSE values follow a similar Pattern, with the largest errors occurring at high-elevation and complex-terrain stations (ex: Ratnapura, Nuwara Eliya, Katugastota, Hambantota). Importantly, within the primary HW hotspot regions of the northern and eastern dry-zones, correlations remain high, and biases remain relatively low, supporting the use of ERA5 T_{max} for the seasonal HW characterization presented in sections 3.2-3.5.

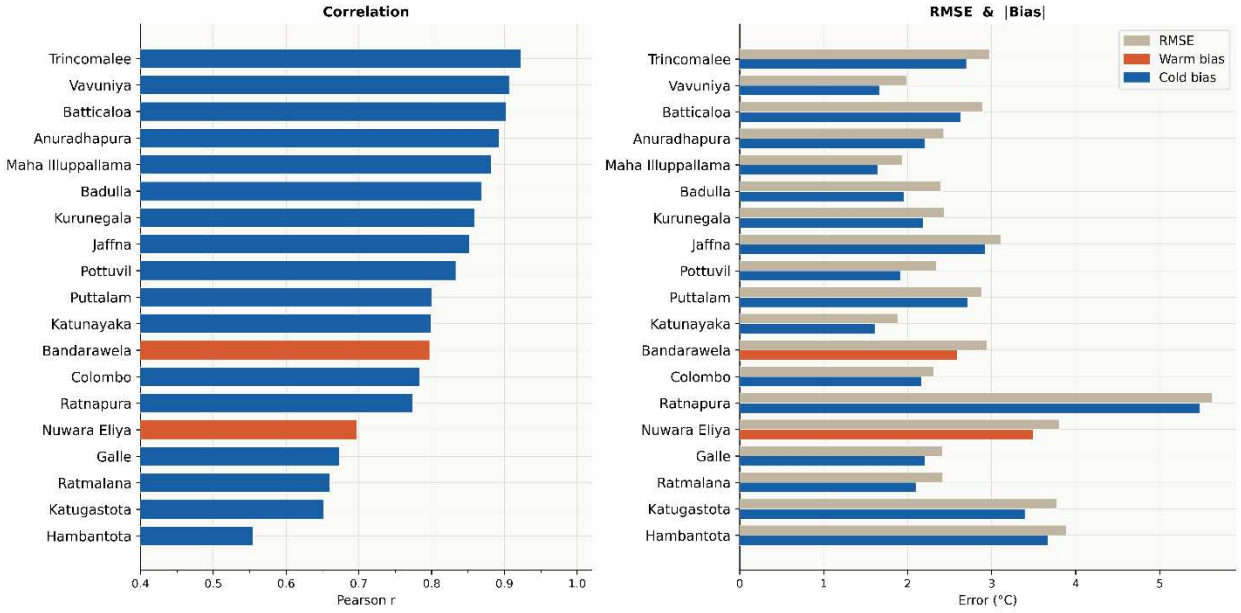


Fig. 2 Validation skill-score summary comparing ERA5 T_{max} against 19 meteorological station observations (1995-2024). (a) Pearson correlation coefficient (r) ranked by station, with warm bias stations shown in orange and cold bias stations in blue. (b) Corresponding RMSE and absolute MB (°C) for each station.

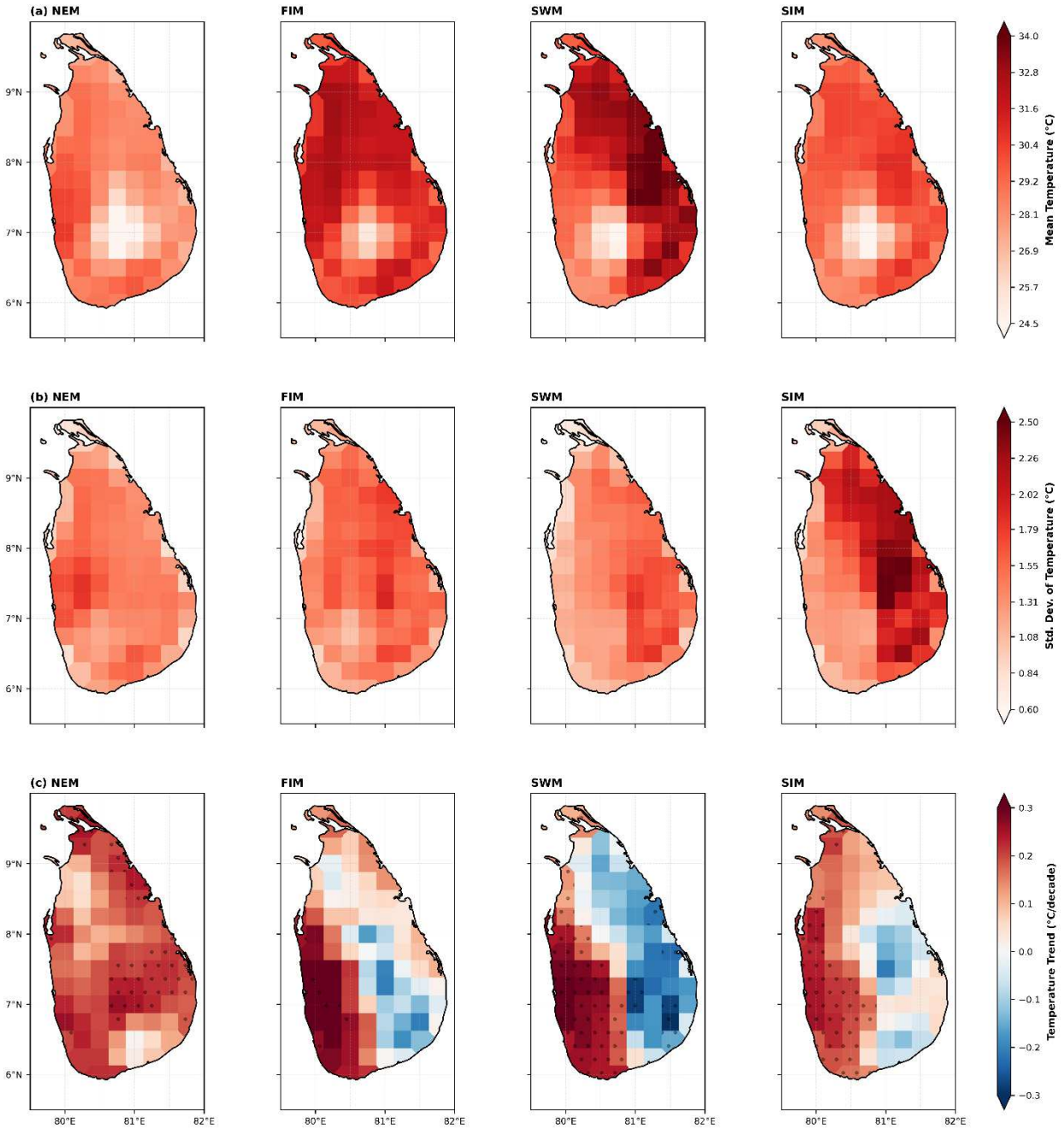
3.2 Seasonal climatology of T_{max}

The spatial distribution of seasonal mean T_{max} over Sri Lanka (Fig. 3a) reflects the combined influence of monsoonal circulation, topography, and the island's tropical setting. A persistent cool

core is evident over the central highlands in all seasons, while warmer conditions dominate the surrounding lowlands. This thermally stratified structure arises primarily from elevation-dependent cooling and orographic control of airflow, which together regulate both temperature and precipitation patterns (Domroes & Ranatunge, 1993; Punyawardena, 2010). Consequently, a marked climatic contrast exists between the humid southwestern highlands and the semi-arid northern and eastern lowlands (Climate Change Secretariat, 2016).

Superimposed on this topographic control, clear seasonal differences emerge. During the NEM season, T_{max} ranges between ~27–30 °C across most regions. Relatively stable atmospheric conditions, moderate cloud cover, and limited convective activity suppress excessive daytime heating, resulting in comparatively moderate temperatures (Suppiah, 1996; Zubair et al., 2008). In contrast, the FIM season represents the annual peak in background thermal conditions. T_{max} exceed 32 °C across extensive areas of the northern, eastern, and southwestern lowlands. This reflects strong solar insolation, weak large-scale circulation, and reduced cloud cover during the pre-monsoon period, which together maximize net surface radiation and promote widespread warming (Karunathilaka et al., 2017).

During SWM, a pronounced east–west contrast develops. The southwestern windward region and central highlands experience lower T_{max} due to persistent cloud cover and rainfall associated with southwesterly monsoon flow. In contrast, the northern and eastern leeward regions remain relatively hot, which may be due to rain-shadow effects, which reduce cloudiness and enhance surface heating. This orographically driven thermal asymmetry is a defining feature of Sri Lanka's climate. The SIM season exhibits moderately high T_{max} but with a more spatially uniform pattern. Increased convective activity and frequent rainfall events associated with transitional atmospheric conditions act to moderate temperatures through enhanced cloud cover and latent heat fluxes, reducing strong spatial gradients. Overall, these results indicate that while topography imposes a persistent spatial structure on T_{max}, seasonal variations are primarily governed by changes in cloud cover, radiative forcing, and monsoonal circulation.



364

365 **Fig. 3 (a)** Seasonal climatology, **(b)** Seasonal variability of maximum temperature (°C), and **(c)**
366 Trends of maximum temperature (°C/ decade) over Sri Lanka for NEM, FIM, SWM, and SIM
367 derived from ERA5.Trends are calculated using Least-Squares Regression of annual seasonal
368 mean temperature. Black dots indicate grid points where the trend is statistically significant at $P <$
369 0.05

370

3.3 Seasonal variability of T_{max}

The seasonal variability of T_{max}, represented by the STD of daily values (Fig. 3b), provides insight into the temporal stability of temperature conditions. The NEM season exhibits the lowest variability (STD < ~1.5 °C), reflecting its relatively stable atmospheric state with limited synoptic disturbances and weak temperature fluctuations (Suppiah, 1996). Variability increases markedly during the FIM season, particularly over the northern and eastern regions. This reflects the transitional nature of the pre-monsoon period, during which alternating clear-sky conditions and episodic convection produce strong fluctuations in radiative forcing and surface temperature (Karunathilaka et al., 2017). This heightened thermal variability during the pre-monsoon season reflects the progressive destabilization of the lower troposphere as solar heating intensifies and low-level moisture increases ahead of the monsoon onset.

During SWM, variability is moderate overall but shows spatial contrasts. The southwestern wet-zone maintains relatively stable T_{max} due to persistent cloud cover and rainfall, while the eastern dry-zone exhibits higher variability linked to intermittent cloud cover and monsoonal break periods. The SIM season displays the highest variability across several regions. Frequent convective events and tropical disturbances introduce substantial day-to-day fluctuations in cloud cover, precipitation, and surface energy balance. As a result, T_{max} variability peaks during this dynamically active transition season. Taken together, these results indicate that inter-monsoon seasons (particularly SIM) are characterized by enhanced thermal variability, whereas monsoon seasons exhibit greater stability due to persistent large-scale circulation patterns.

3.4 Long-term Trends in T_{max}

The spatial patterns of long-term trends in seasonal T_{max} (1995-2024; Fig. 3c) reveal substantial regional and seasonal heterogeneity. A coherent and statistically significant warming signal emerges during the NEM season across most parts of the country, particularly in the northern and eastern regions, with trends exceeding ~0.2 °C/decade. This aligns with broader large-scale warming patterns (IPCC, 2023a) and may partly reflect the influence of rapid warming in the tropical Indian Ocean, which alters the regional atmospheric circulation (Roxy et al., 2014, 2015).

In contrast, the FIM season displays a more spatially heterogeneous trend pattern, with warming in western and southern regions and weaker or locally negative trends in parts of the east. This suggests a stronger influence of local processes, including cloud variability, land–atmosphere coupling, and regional circulation anomalies. During SWM, the trend pattern shows a pronounced west-east asymmetry. Significant warming occurs in the western and southwestern regions, while eastern areas show weaker trends or slight cooling. These differences are likely linked to changes in monsoon rainfall distribution and cloud cover, which modulate surface radiative heating. During the SIM season, moderate warming occurs in the western and southern regions, while elsewhere, patterns are less coherent. This reflects the complex interaction between convective activity and ocean–atmosphere variability during the transition period.

Overall, T_{max} warming is evident across Sri Lanka, but it is strongly season-dependent. These differences emphasize the importance of monsoonal circulation and ocean–atmosphere interactions in shaping regional temperature trends. Notably, these climatological changes establish the baseline conditions upon which HW characteristics develop.

3.5 Seasonal Characteristics of Heat Waves over Sri Lanka

3.5.1 Seasonal frequency and proportional contribution

The seasonal distribution of HW frequency across Sri Lanka is presented in Fig 4a. In terms of absolute event count, the highest number of detected HWs occurs during SWM, particularly over northern, northwestern, eastern, and southeastern lowlands. In contrast, the SIM exhibits the lowest HW frequency across most regions, while the NEM and the FIM show intermediate patterns. However, because SWM spans five months, raw event counts alone overestimate its relative importance. When normalized by season length (Fig. 4b), a different picture emerges: the FIM season shows the highest proportion of HW days. This indicates that extreme heat occupies a larger fraction of the seasonal climate during FIM, despite fewer total events.

This distinction reveals two complementary aspects of HW behaviour: SWM is the highest cumulative event count, while FIM is the strongest dominance of HWs within the season. Both metrics consistently identify the northern, eastern and south-eastern dry-zones as hotspots, while the central highlands are least affected due to their elevation and the influence by clouds. The

prominence of FIM is physically linked to strong insolation, weak atmospheric ventilation and limited cloud development, which favour rapid boundary-layer warming and frequent threshold exceedance.

A sensitivity analysis using an alternative 90th percentile threshold (Fig. S2) resulted in higher HW frequencies across all seasons, as expected from the lower exceedance threshold. However, the overall spatial distribution of HW activity remained remarkably similar. The northern, eastern, and southeastern dry-zone lowlands consistently emerged as the dominant hotspot regions under both threshold definitions, while the central highlands remained comparatively less affected. This indicates that the identified hotspot patterns are robust and are not strongly dependent on the choice of percentile threshold.

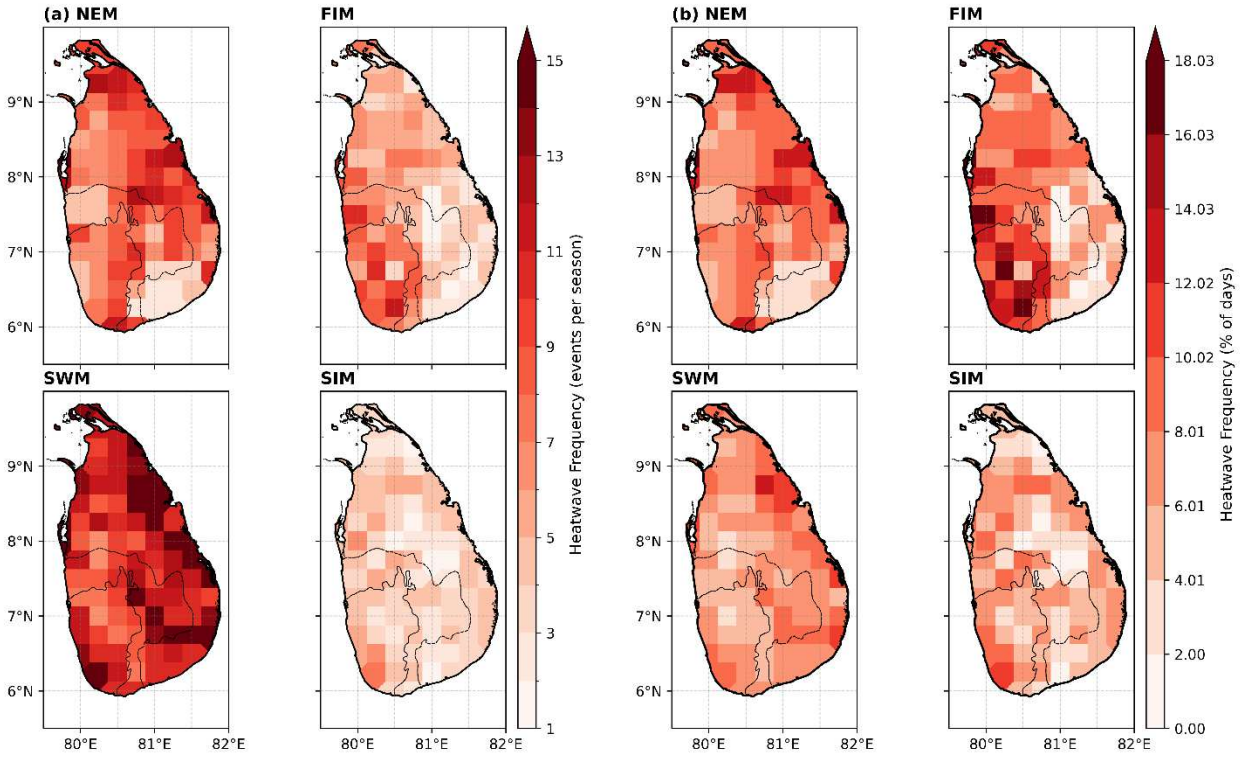


Fig. 4 (a) Seasonal distribution of Heat Wave (HW) Frequency (Total number of events per season) across Sri Lanka, **(b)** Seasonal distribution of HW Frequency (% of days) across NEM, FIM, SWM, and SIM, derived from ERA5

3.5.2 Heat Wave Intensity

The maximum HW intensity during the study period, defined as the highest daily T_{max} recorded within any HW event at each grid point is presented in Fig. 5a. The maximum HW intensity is highest in the dry-zone lowlands, particularly during FIM and SWM. In contrast, the central highlands display relatively low temperatures, indicating that even the most intense HW events are substantially reduced by elevation-induced thermodynamic constraints. FIM exhibits the most extensive and severe intensities, reflecting its high background T_{max}. This is consistent with the seasonal mean T_{max} (Fig. 3a) patterns discussed in section 3.2, where FIM was identified as the period of peak background thermal conditions over large parts of Sri Lanka. Elevated climatological baseline implies that even moderate anomalies translate into very high absolute temperatures. As a result, FIM not only shows a high proportional contribution (Fig. 4b), but also thermally extreme.

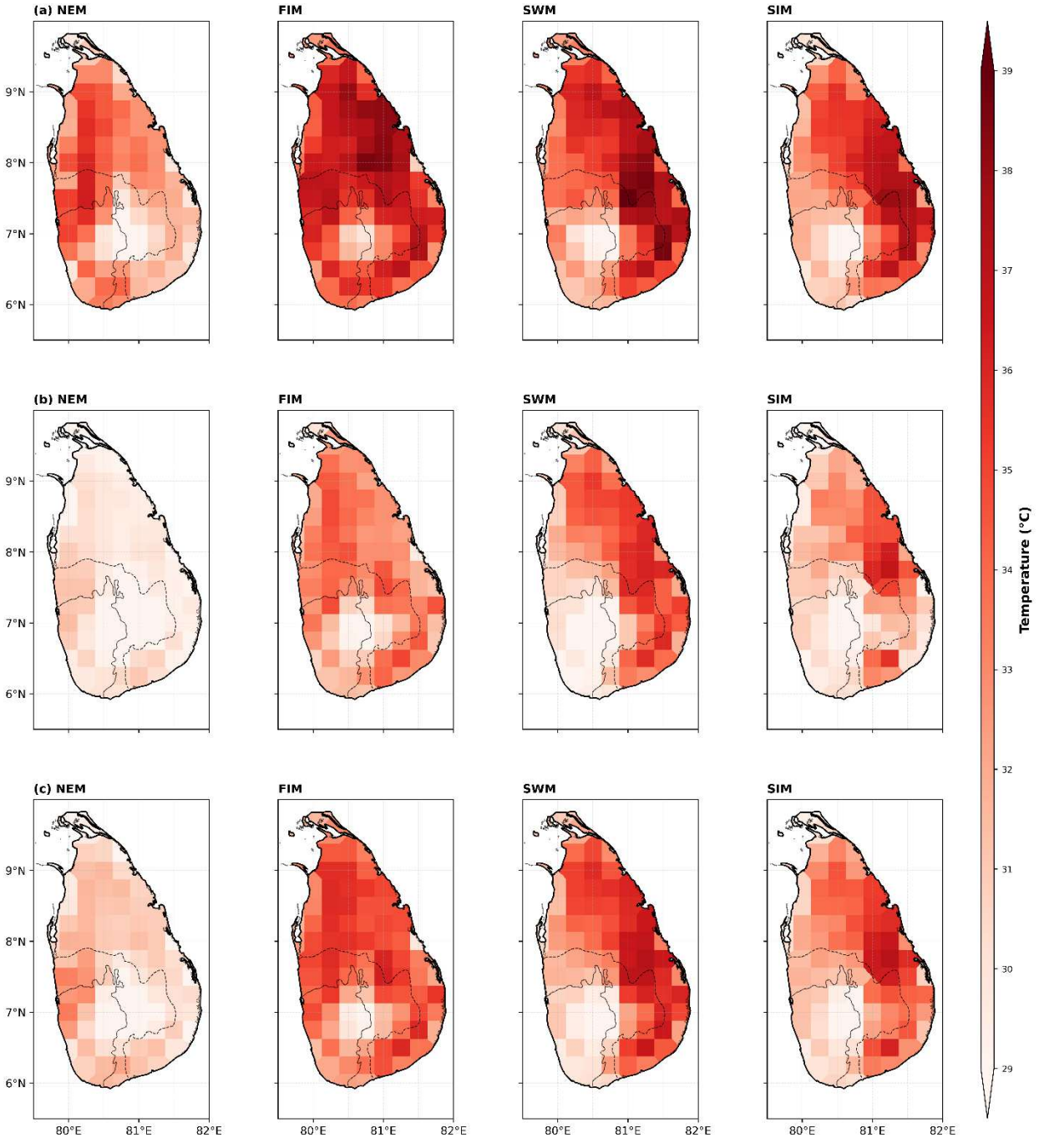
During SWM, high intensities persist in leeward eastern regions, consistent with the well-documented rain-shadow influence of Sri Lanka's central highlands during the SWM (Domroes & Ranatunge, 1993; Karunathilaka et al., 2017). The SIM shows moderate intensities, and NEM exhibits weaker intensities due to convective interruptions. Thus, the maximum intensity maps suggest that the strongest HW conditions are concentrated in the dry-zone lowlands, while the impact intensifies during FIM compared to other seasons.

The seasonal distribution of minimum (Fig. 5b) and mean (Fig. 5c) intensity reveals the sustained thermal nature of HWs. Dry-zone regions experience high minimum intensities, especially during FIM and SWM. This indicates that even the least intense days within these events remain unusually warm. This reflects an overall shift upwards in the temperature distribution. In contrast, the central highlands and parts of the southwestern wet-zone exhibit markedly lower minimum intensities. This spatial contrast in minimum intensity has direct physical significance: a high thermal floor implies that the entire duration of a HW in the dry-zone lowlands is characterized by sustained warmth rather than alternating between brief extremes and near-normal temperatures.

Mean intensity patterns (Fig. 5c) closely mirror seasonal mean T_{max} (Fig. 3a), confirming that background climatology exerts a strong influence on event severity. This is consistent with the broader understanding that, in tropical climates where inter-annual temperature variability is relatively low, even modest positive anomalies relative to a warm seasonal mean can generate substantial events (Perkins-Kirkpatrick & Lewis, 2020; IPCC, 2023a). FIM emerges again as the

474 dominant season for sustained heat, followed by SWM in leeward regions. These results
475 demonstrate that dry-zone HWs are not only intense but also persistently warm throughout their
476 duration, thereby increasing cumulative thermal stress.

477



478

Fig. 5 Seasonal distribution of **(a)** Maximum HW Intensity (°C), **(b)** Minimum HW Intensity (°C), and **(c)** Mean HW Intensity (°C) across Sri Lanka for NEM, FIM, SWM, and SIM, derived from ERA5.

3.5.3 Heat Wave Duration

The spatial distributions of the strongest and mean HW duration are presented in Fig. 6a and Fig. 6b, respectively. The strongest duration metric (Fig. 6a) shows that the longest HW events occur mainly during FIM and SWM, with the highest persistence concentrated over the eastern, southeastern, and parts of the north-central dry-zone lowlands. In several locations, individual events persist for more than 10 days, indicating prolonged HW conditions are a prominent feature of the country. During FIM, prolonged HW events are spatially widespread across much of the central region and dry-zone. SWM also exhibits pronounced HW persistence, although the longest events are more spatially confined to the eastern and southeastern lowlands. In contrast, the central highlands consistently show much shorter event durations in NEM and SIM. The SIM season generally displays shorter HW durations across most parts of the island, while NEM exhibits moderate persistence, mainly over the northern dry-zone regions. Overall, the strongest-duration patterns indicate that the most persistent HW events in Sri Lanka are concentrated in the dry-zone lowlands during FIM and in the eastern leeward regions during SWM.

The mean duration metric (Fig. 6b) complements the strongest-duration analysis by representing the typical persistence of HW events rather than isolated extremes. Mean HW duration is generally highest during FIM, particularly across the north-central, eastern, and southeastern parts of the island, indicating that HWs during this season are not only frequent and intense but also systematically long-lasting. Although SWM records a larger number of HW events overall, this is partly related to the longer duration of the monsoon season itself.

Taken together, the strongest and mean duration metrics consistently identify the eastern and southeastern dry-zones as the principal regions of persistent HW activity in Sri Lanka. More broadly, the results reveal a spatially coherent pattern of HW behaviour across the island. The dry-zone lowlands consistently experience the highest HW frequency, intensity, and persistence, while the central highlands remain comparatively less affected. Among the four seasons, FIM emerges

as the most HW-dominated season in relative terms, characterized by high proportional HW occurrence, elevated intensity, and long event duration. SWM records the highest absolute number of events, with particularly persistent HW conditions over the eastern and southeastern regions. In contrast, NEM and SIM exhibit comparatively weaker HW activity. These findings highlight the strong spatial and seasonal variability of HW characteristics across Sri Lanka.

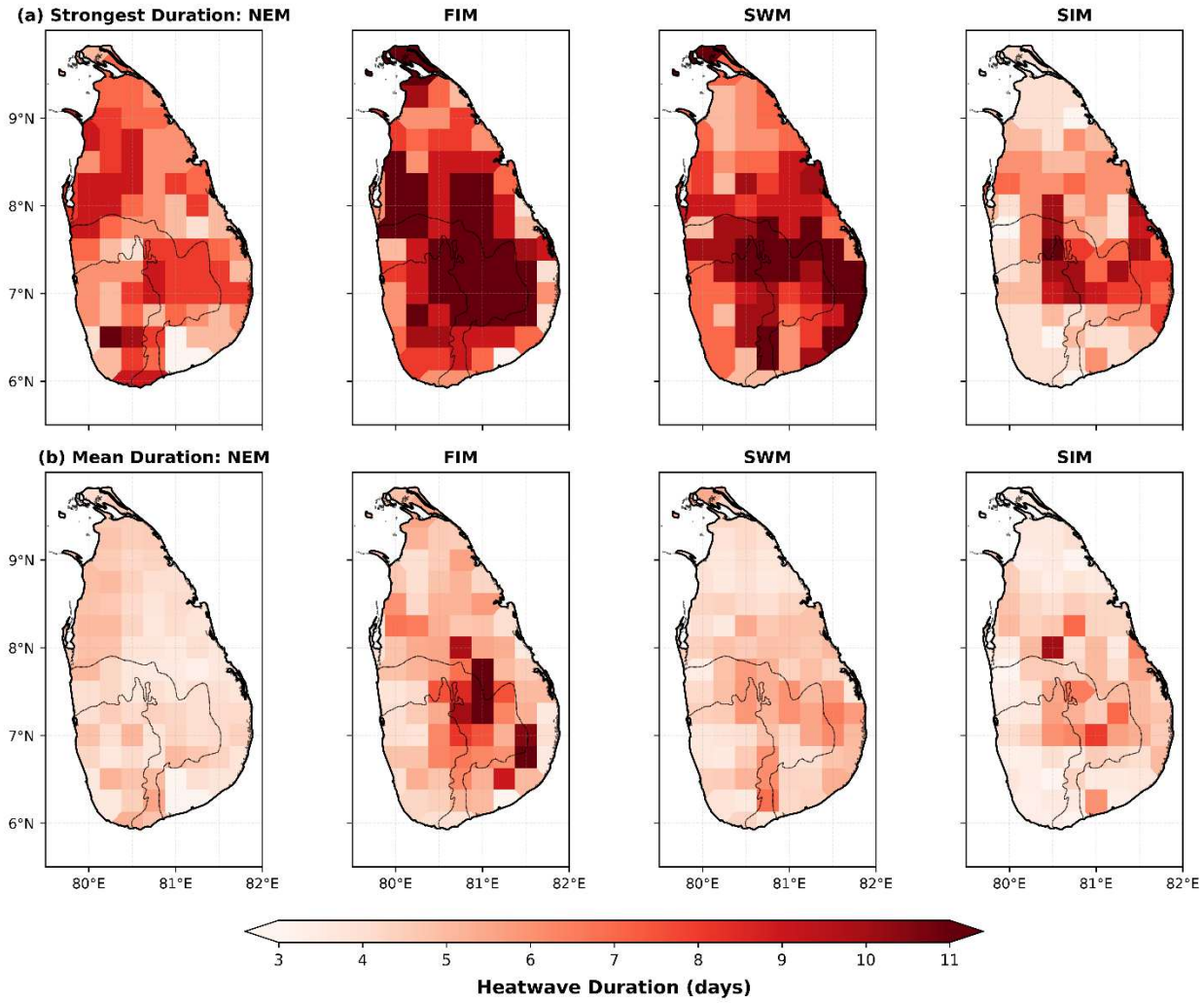


Fig. 6 Seasonal distribution of Heat Wave **(a)** Strongest Duration and **(b)** Mean Duration across Sri Lanka throughout the NEM, FIM, SWM, and SIM derived from ERA5

3.5.4 Heat Wave Metrics Trends

The trend analysis of HW metrics reveals a non-uniform and seasonally dependent evolution of extreme temperature behaviour, which contrasts with the more coherent warming signal observed in seasonal mean temperatures. This indicates that changes in HW characteristics are not simply a linear response to background warming.

All monsoonal seasons exhibit weak positive trends in HW frequency over the study period (Table S3), suggesting a gradual increase in the occurrence of extreme temperature events. The strongest increase is observed during the SWM, followed by the SIM, while weaker increases are observed during the NEM and FIM. However, none of these trends are statistically significant, indicating that interannual variability dominates the long-term signal in HW occurrence.

HW intensity shows a clearer seasonal signal. The NEM exhibits a statistically significant decreasing trend in maximum intensity (slope = -0.1829 °C/year, $p = 0.025$) indicating a robust reduction in peak HW severity during this season. Other seasons show weak and non-significant trends, with SWM displaying a decreasing tendency, SIM a slight increase, and FIM remaining nearly stable. This suggests that intensity changes are strongly seasonally asymmetric, with only NEM showing a statistically robust signal (Table S3).

Trends in strongest HW duration are generally weak and statistically insignificant across all seasons. The SWM shows the largest positive slope, suggesting a possible increase in persistence of extreme events, while FIM shows a slight negative trend. NEM and SIM exhibit weak positive tendencies. Overall, there is no statistically robust evidence of a consistent long-term change in HW duration during the study period (Table S3).

4 Discussion

4.1 Atmospheric and Oceanic Drivers of Seasonal Heat Waves over Sri Lanka

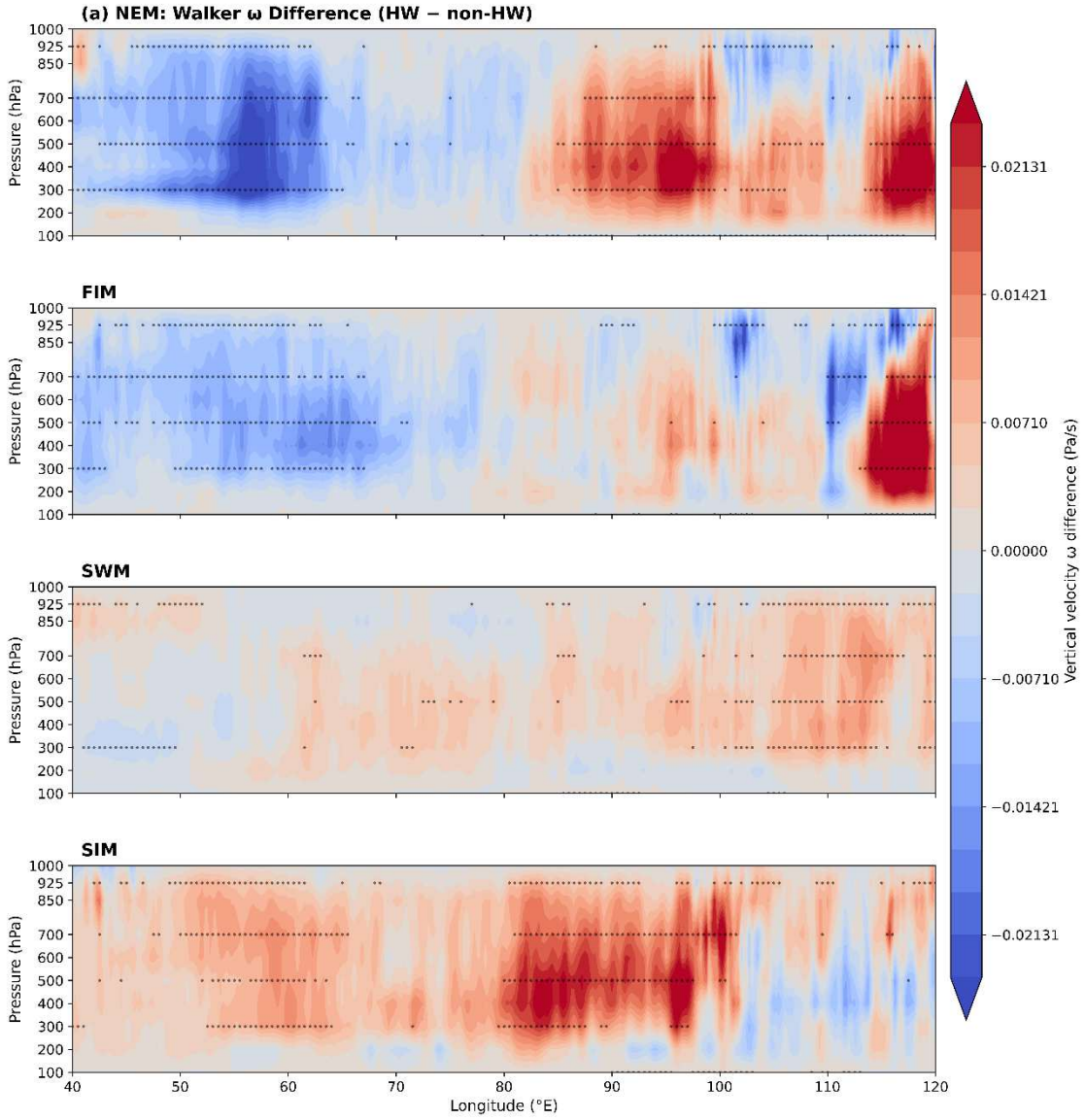
4.1.1 Large-Scale Circulation Background and Anomalous Subsidence

Sri Lankan HWs develop within the broader dynamical framework of the Walker and Hadley circulations over the tropical Indian Ocean. Climatologically, the Walker circulation is characterized by enhanced ascent over the eastern Indian Ocean and Maritime Continent and subsidence toward the western basin (Fig. S3a), while the Hadley circulation exhibits tropical

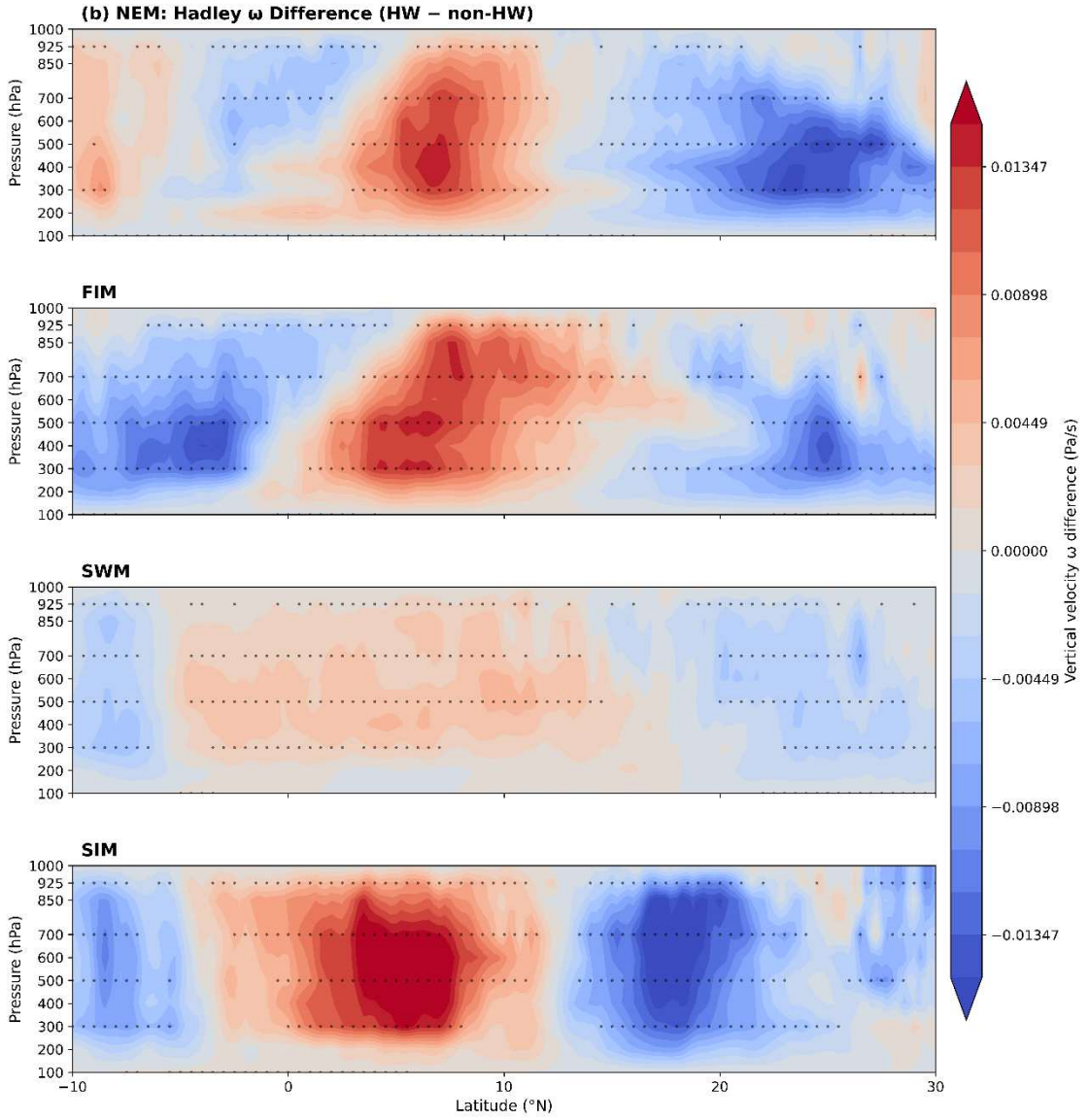
ascent and subtropical descent (Fig. S3b). Sri Lanka lies near the transition zone between these ascending and descending branches, making the island highly sensitive to changes in regional vertical motion.

Composite differences between HW and non-HW conditions reveal that HW days are consistently associated with enhanced subsidence across the northern Indian Ocean (Fig. 7). Positive vertical velocity anomalies indicate stronger downward motion during HW periods, implying a large-scale suppression of atmospheric convection. Such subsidence promotes atmospheric stability, reduces cloud formation and favours increased surface heating, consistent with mechanisms identified in previous HW studies (Trenberth & Fasullo, 2012; Perkins-Kirkpatrick & Lewis, 2020).

The spatial structure of the subsidence signal varies seasonally. During FIM, the anomalous subsidence is spatially coherent and extends across much of the northern Indian Ocean and Sri Lanka, supporting island-wide HW development. In contrast, the SWM season exhibits weaker and more spatially heterogeneous subsidence anomalies, suggesting that local and regional processes become increasingly important during this season. This seasonal contrast helps explain why FIM HWs are widespread across the island, whereas SWM HWs are concentrated mainly in the eastern and south-eastern dry-zone lowlands.


(a) NEM: Walker ω Difference (HW − non-HW)
FIM
SWM
SIM
Pressure (hPa)
1000
925
850
700
600
500
400
300
200
100
40
50
60
70
80
90
100
110
120
Longitude (°E)
0.02131
0.01421
0.00710
0.00000
−0.00710
−0.01421
−0.02131
Vertical velocity ω difference (Pa/s)

563



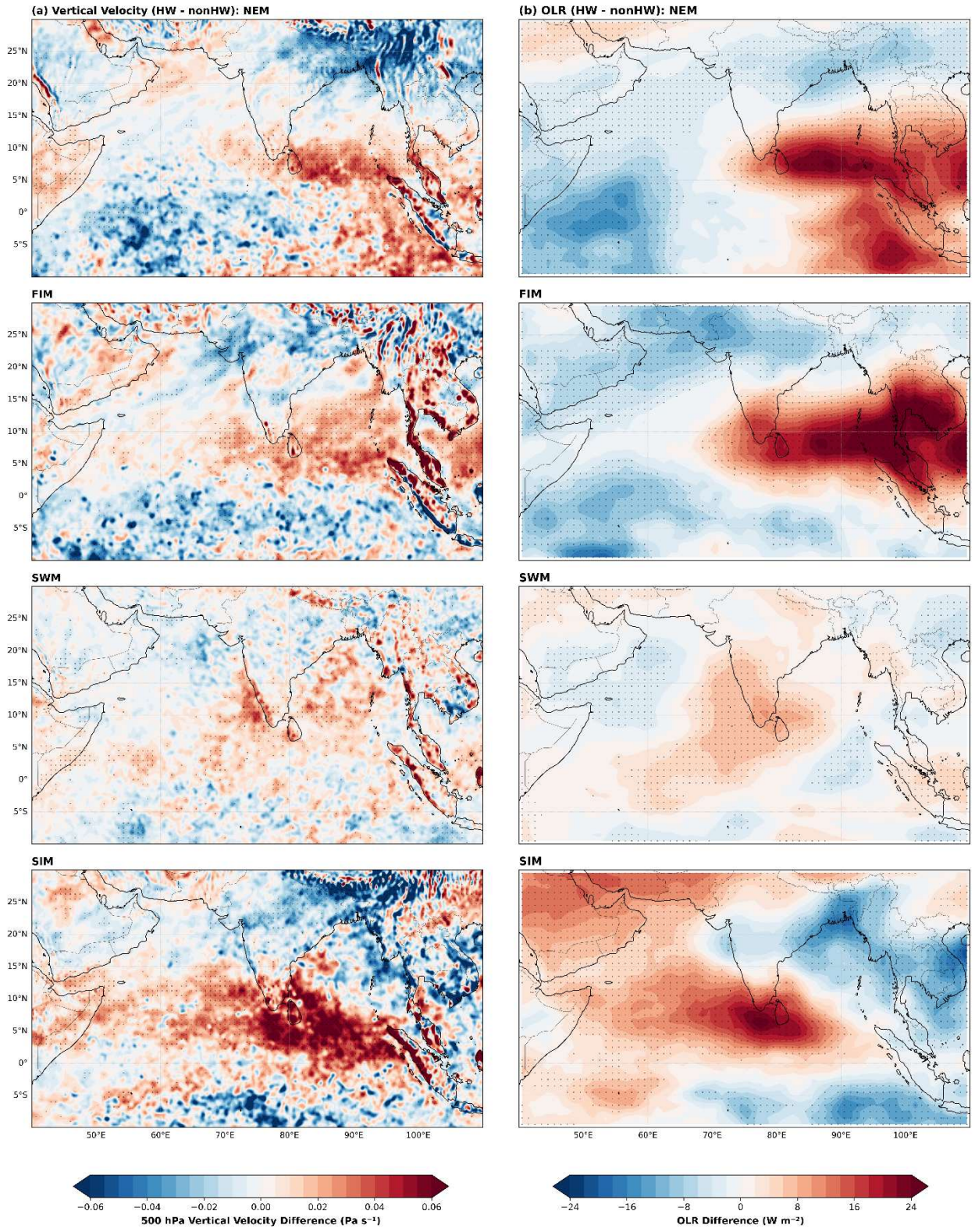
564

565 **Fig. 7 (a)** Seasonal differences in the Walker circulation between HW and non-HW conditions
566 over the tropical Indian Ocean (40°E–120°E). The panels show the vertical velocity difference (ω;
567 Pa/s) in the longitude–pressure plane and **(b)** Seasonal differences in the Hadley circulation
568 between HW and non-HW conditions over the tropical Indian Ocean (10S-30N). The panels show
569 the vertical velocity difference (ω; Pa/s) in the latitude–pressure plane for NEM, FIM, SWM, and
570 SIM. Negative values indicate enhanced ascending motion during HW periods, while positive
571 values represent stronger subsidence during HW conditions relative to non-HW periods. Stippling
572 denotes grid points where the difference is statistically significant at the 5% level (Welch's t-test)

573 **4.1.2 Mid-Tropospheric Vertical Velocity, Convective Suppression, and OLR anomalies**

The role of atmospheric subsidence is further confirmed by the 500 hPa vertical velocity and OLR composites (Fig. 8a and Fig.8b respectively). Positive 500 hPa ω anomalies during HW days indicate enhanced mid-tropospheric downward motion over Sri Lanka and the surrounding oceanic region. At the same time, positive OLR anomalies reveal reduced convective cloudiness and enhanced clear-sky conditions.

These two variables together provide strong evidence that HW events are closely linked to suppressed convection. Reduced deep convection limits cloud development and precipitation, resulting in greater solar heating of the land surface. The strongest and most spatially coherent positive OLR anomalies occur during the inter-monsoon period, indicating that inter-monsoon HWs are particularly associated with large-scale convective suppression across the northern Indian Ocean. This relationship between subsidence and reduced convection is particularly important in tropical climates such as Sri Lanka, where relatively small perturbations in cloud cover can strongly modify the surface energy balance. The broad spatial coherence of these anomalies during the FIM helps explain the widespread and proportionally dominant HW conditions identified above.



589

590 **Fig. 8** Composite differences in **(a)** 500 hpa vertical velocity ω (Pa/s), between HW and non-HW

591 days. Positive values indicate anomalously stronger subsidence on heat wave days. **(b)** OLR (W

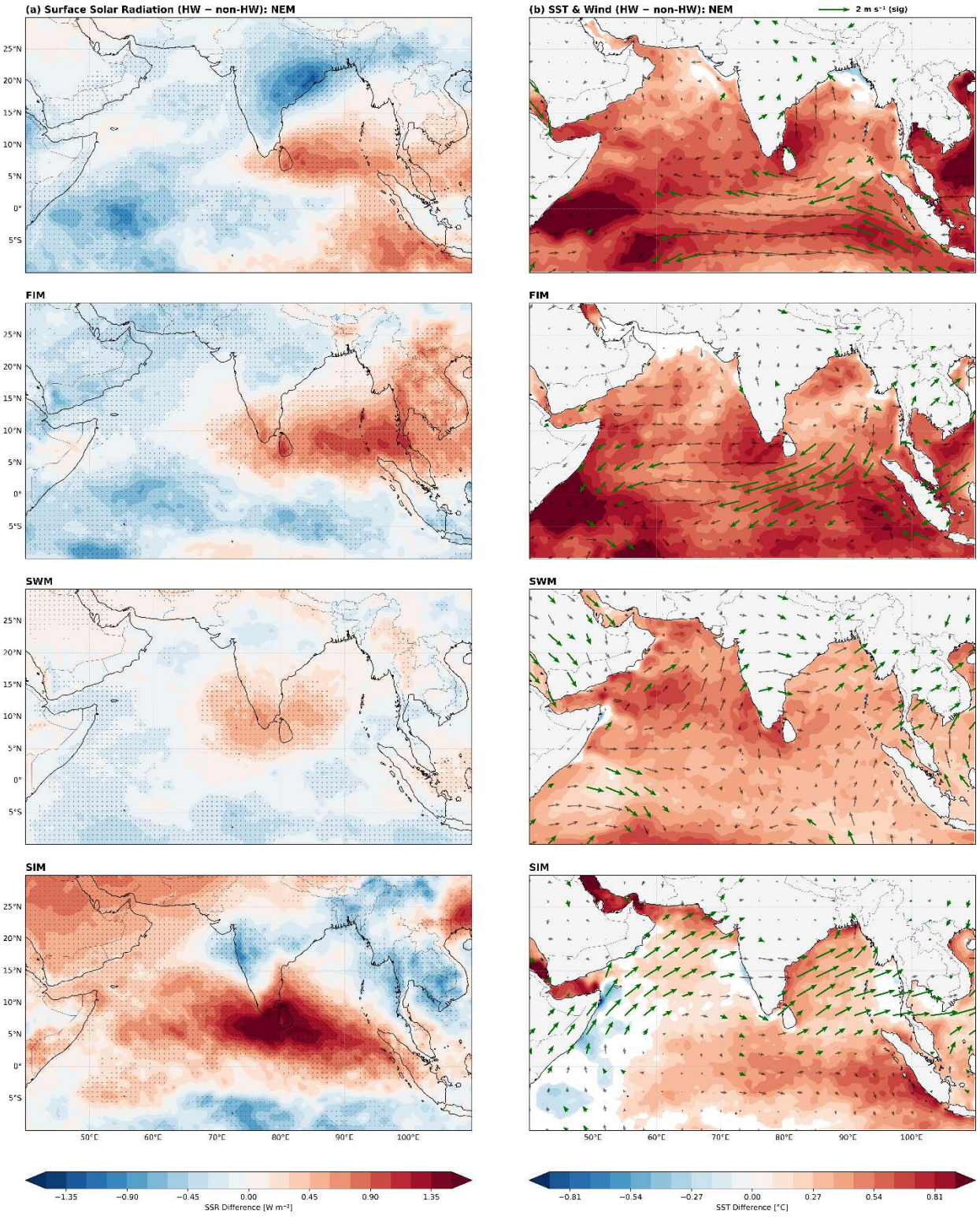
592 m^{-2}) between HW and non-HW days. Stippling denotes grid points where the difference is
593 statistically significant at the 5% level (Welch's t-test)

594

595 **4.1.3 Cloud Dynamics and Shortwave Radiation Amplification**

596 The suppression of convection during HW periods is directly reflected in reductions in both HCC
597 and LCC (Fig. S4). Negative cloud-cover anomalies are accompanied by positive anomalies in
598 downward shortwave radiation (Fig. 9a), indicating enhanced solar energy reaching the surface
599 during HW days. This radiative response represents a key amplification mechanism for HW
600 development. In Sri Lanka's tropical environment, solar radiation is a dominant component of the
601 surface energy budget (Renne et al., 2003); therefore, reductions in cloud shading rapidly increase
602 land-surface heating and near-surface air temperature.

603 The spatial expression of this radiative amplification differs markedly between seasons. During
604 FIM, positive Shortwave Radiation anomalies extend across much of the island, consistent with
605 the widespread HW activity observed during this season. During SWM, however, enhanced
606 Shortwave Radiation is mainly confined to the eastern and southeastern dry-zone lowlands. This
607 reflects the strong topographic influence of the central highlands, which intercept moist
608 southwesterly monsoon flow and maintain persistent cloudiness over the southwestern windward
609 region while allowing clearer conditions to persist in the leeward east. The combined reduction in
610 cloud cover and increase in Shortwave Radiation therefore provide the immediate surface-energy
611 pathway linking large-scale subsidence to extreme surface heating.



612

613 **Fig. 9** Composite differences in **(a)** Shortwave Radiation (W m^{-2}), and **(b)** SST (C °) & 10-m Wind

614 vectors between HW and non-HW days. Panel (a) shows Positive values indicate increased

615 downward shortwave radiation at the surface during heat wave conditions. Stippling denotes grid
616 points where the difference is statistically significant at the 5% level (Welch's t-test). Panel (b)
617 Shading shows only statistically significant SST differences ($p < 0.05$, Welch's t-test). Green
618 arrows indicate statistically significant wind differences at $p < 0.05$ (both u- and v-components);
619 black arrows show non-significant wind differences

620

621 **4.1.4 Basin-scale Ocean-atmosphere Coupling**

622 The SST and 10-m wind composites (Fig. 9b) indicate that Sri Lankan HWs occur within a broader
623 warm Indian Ocean environment. Positive SST anomalies are evident across large sectors of the
624 tropical Indian Ocean during HW periods, suggesting that oceanic conditions provide an important
625 background state for HW development.

626 These warm SST anomalies likely reinforce the atmospheric conditions favourable for HWs by
627 supporting a warmer lower troposphere and modifying regional circulation patterns. The influence
628 of rapid Indian Ocean warming on atmospheric circulation and South Asian climate has been
629 widely documented (Roxy et al., 2014; Xie et al., 2016), and the present results suggest that Sri
630 Lankan HWs are embedded within this broader ocean-atmosphere system. The SST influence
631 appears strongest during FIM, when warm oceanic conditions coincide with the seasonally
632 warmest continental temperatures. During SWM, SST anomalies remain positive, but the spatial
633 distribution of HW activity over Sri Lanka is more strongly controlled by topography and
634 monsoonal circulation. These findings indicate that warm Indian Ocean SSTs act primarily as a
635 reinforcing boundary condition rather than as a direct trigger of HWs.

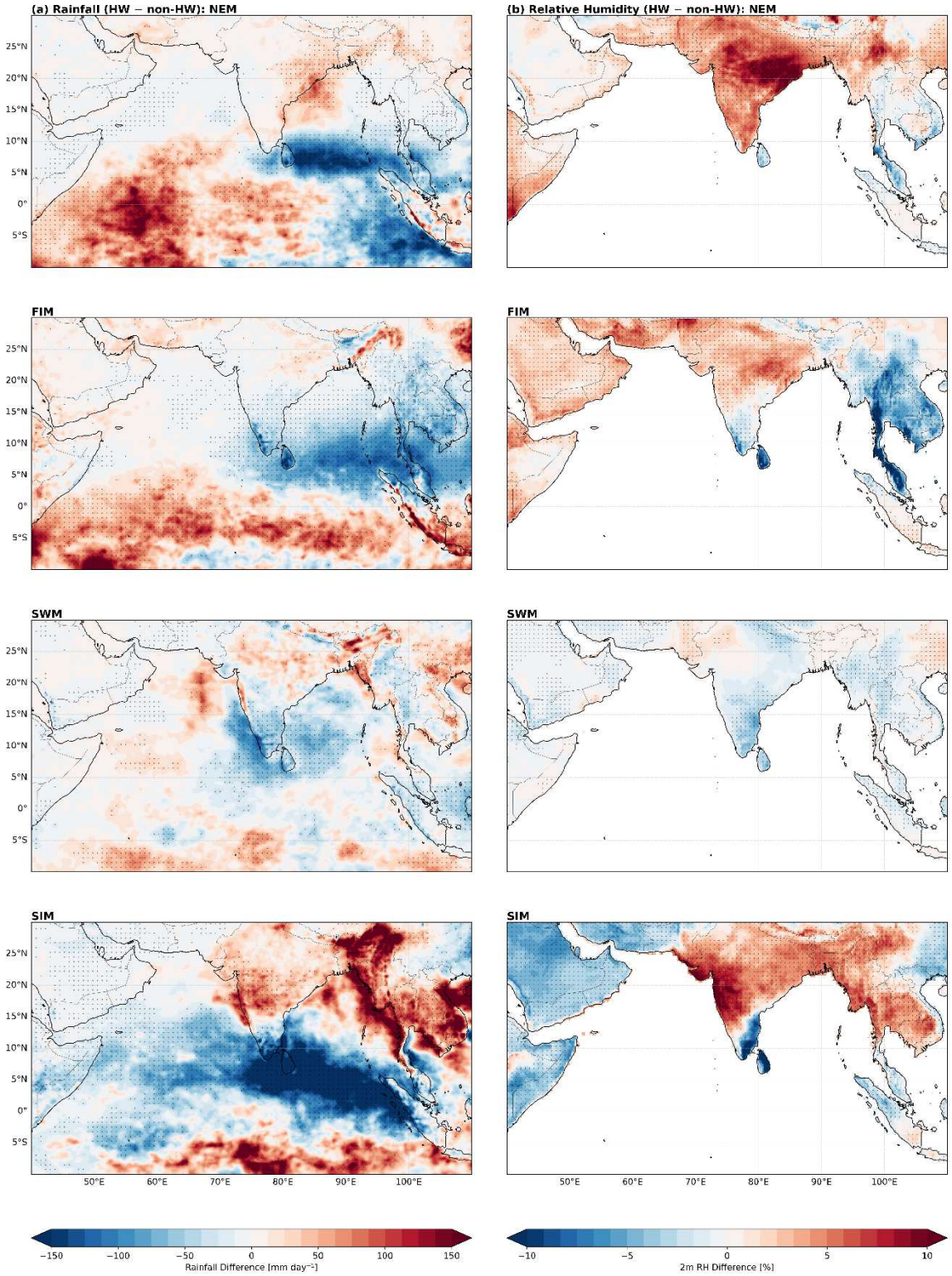
636

637 **4.1.5 Hydro-Climatic Feedbacks: Rainfall Deficits and Boundary-layer Humidity**

638 HW days are also characterized by substantial reductions in rainfall (Fig. 10a) and RH (Fig. 10b).
639 Negative rainfall anomalies indicate that HW events occur under anomalously dry conditions,
640 while reduced RH reflects drying of the lower atmosphere and land surface (Zscheischler et al.,
641 2020). These hot-dry conditions likely enhance HW persistence by reducing evaporative cooling
642 and increasing the proportion of available surface energy converted into sensible heating (Chen et

al., 2026). Such land-atmosphere feedback processes are widely recognized as important amplifiers of extreme heat and compound drought-heat events (Seneviratne et al., 2010; Miralles et al., 2014).

The strongest RH reductions occur during FIM and over the eastern and southeastern dry-zone lowlands, consistent with the regions identified as HW hotspots. This indicates that boundary-layer drying contributes not only to higher daytime temperatures but also to the maintenance of persistently warm conditions throughout HW events (Jackson et al., 2025). The co-occurrence of HW conditions with rainfall suppression and atmospheric drying has important implications for Sri Lanka because it links thermal stress directly with water stress (Li et al., 2025). These compound hot-dry conditions are particularly relevant for agriculture, irrigation demand, and human health in the dry-zone regions of the country.



654

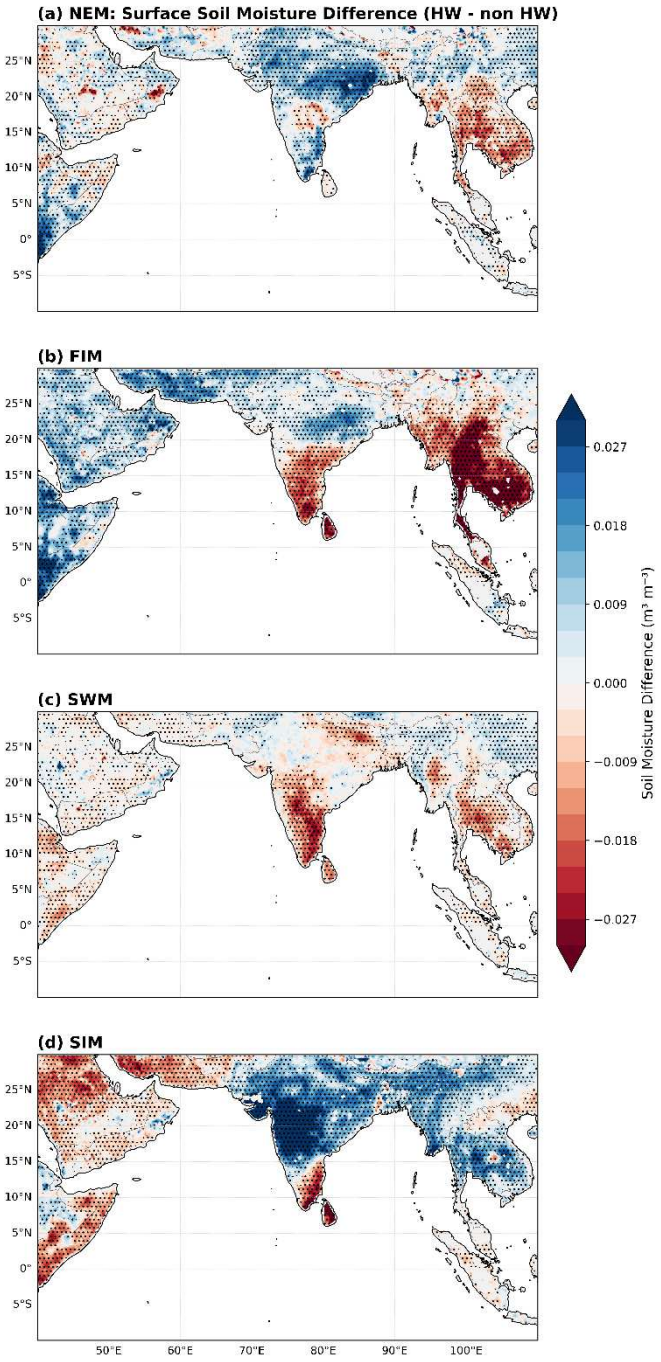
655 **Fig. 10** Composite differences in **(a)** Total Rainfall (mm/day), and **(b)** RH (%) between HW and
656 non-HW days. Stippling denotes grid points where the difference is statistically significant at the
657 5% level (Welch's t-test)

4.1.6 Land-Surface Desiccation and Soil Moisture-Temperature Coupling

The surface soil moisture composites provide further evidence that land-surface drying is closely associated with HW conditions across Sri Lanka (Fig. 11). Negative surface soil moisture anomalies indicate that HW days generally occur under drier surface conditions than non-HW days, supporting a coupling between land-surface moisture availability and near-surface temperature. As soil moisture declines, the capacity of the land surface to dissipate available energy through evapotranspiration is reduced, favouring a greater partitioning of energy toward sensible heating. Such soil moisture–temperature coupling is a well-established mechanism for amplifying warm extremes, particularly when strong radiative forcing coincides with limited water availability (Miralles et al., 2014; Chen et al., 2026).

The strength and spatial extent of this relationship vary substantially between seasons. During FIM, negative soil moisture anomalies extend across much of Sri Lanka (Fig. 11b), coinciding with the widespread HW activity and strong radiative forcing identified above. The spatial coherence suggests that land-surface drying contributes to the broad regional expression of the FIM HW regime. During SWM, by contrast, soil-moisture anomalies are generally weaker and more spatially heterogeneous (Fig. 11c). This indicates that the active SWM maintains relatively greater land-surface moisture even during HW conditions, particularly outside the leeward dry-zone. The persistence of HWs in the eastern and southeastern lowlands despite this relatively weaker soil-moisture deficit therefore suggests that SWM HWs depend less on widespread land-surface desiccation and more strongly on the regional distribution of moisture and cloud cover associated with the monsoon and topography.

During SIM, negative soil-moisture anomalies are again more spatially coherent over Sri Lanka (Fig. 11d), broadly consistent with the concurrent rainfall deficits, reduced humidity, and enhanced radiative forcing. NEM shows a comparatively weaker and more spatially variable soil-moisture response. Overall, the soil-moisture results indicate that land-surface drying is an important component of the HW environment, but its contribution is seasonally dependent. The particularly strong FIM signal supports a coupled radiative–land-surface pathway, whereas the weaker SWM response highlights the importance of distinguishing the underlying mechanisms of the two major seasonal HW regimes.



687

688 **Fig. 11** Composite differences in Surface Soil Moisture (m^3 m^{-3}) between HW and non-HW days
689 for (a) NEM, (b) FIM, (c) SWM, and (d) SIM. Stippling denotes grid points where the difference
690 is statistically significant at the 5% level (Welch's t-test).

691

692

4.1.7 Reliability of ERA5 T_{max} for Heat Wave Analysis

The reliability of ERA5 maximum temperature for identifying HW variability is supported by the station-based validation presented in Section 3.1. Correlations between ERA5 and observed daily T_{max} exceed 0.80 at most stations and 0.90 at several dry-zone stations, indicating that ERA5 captures the temporal evolution of temperature variability across most of Sri Lanka. This level of agreement is particularly relevant to the present analysis because HWs are identified from persistent departures from the local temperature climatology rather than from isolated absolute temperature values.

The validation nevertheless reveals an elevation-dependent component to the ERA5 temperature bias. Stations in the central highlands generally show a warm bias, whereas some low-elevation stations exhibit a cold bias. These differences are likely related to the 0.25° spatial resolution of ERA5, which cannot fully represent the steep elevation gradients and complex terrain of Sri Lanka. A single grid cell may encompass substantial differences in elevation and land-surface characteristics, resulting in an imperfect representation of local temperature conditions. Such limitations are particularly important when interpreting the magnitude of HW intensity over mountainous areas.

However, the main HW hotspots identified in this study are concentrated in the northern, eastern, and southeastern dry-zone lowlands, where the station validation indicates relatively strong agreement between ERA5 and observations. Moreover, the use of a grid-point-specific percentile threshold reduces the influence of systematic mean temperature biases because HW identification is based on departures from the local climatological distribution. Consequently, although some uncertainty remains in the absolute magnitude of T_{max}, particularly over complex terrain, the principal spatial patterns and seasonal contrasts in HW occurrence are less sensitive to these biases.

The robustness of the identified hotspots is further supported by the threshold sensitivity analysis. Increasing the threshold from the primary 95th percentile to the 90th percentile changes the absolute number of detected events, as expected, but does not substantially alter their spatial distribution. The northern, eastern, and southeastern dry-zone lowlands remain the dominant hotspots. This consistency indicates that the principal geographic features of Sri Lankan HW variability are unlikely to be an artefact of the selected percentile threshold. Together, the station validation and sensitivity analysis provide reasonable confidence that ERA5 is suitable for examining the spatial

and seasonal characteristics and large-scale drivers of HWs across Sri Lanka, while results over complex terrain should be interpreted with greater caution.

4.2 Implications for Climate Risk and Adaptation in Sri Lanka

This study provides the first comprehensive seasonal assessment of HW characteristics and their physical drivers over Sri Lanka, directly addressing the knowledge gap identified in Sri Lanka's Third National Communication (Climate Change Secretariat, 2023). The results demonstrate that HW risk is not spatially uniform across the island. The eastern, southeastern, and north-central dry-zone lowlands consistently experience the highest HW frequency, intensity, and persistence, while the central highlands remain comparatively less affected. Importantly, the FIM and SWM seasons together expose these dry-zone regions to HW conditions over a substantial fraction of the annual cycle.

These findings have direct implications for public health, agriculture, water resources, and energy management. The co-occurrence of extreme heat with rainfall deficits and low humidity suggests that HW periods are also associated with enhanced drought stress, increasing pressure on irrigation systems, reservoir storage, and hydroelectric generation (Zscheischler et al., 2020). The results are therefore highly relevant for climate adaptation planning in Sri Lanka, particularly in sectors identified as climate-sensitive in national adaptation strategies (Climate Change Secretariat, 2023). The identification of warm Indian Ocean SST anomalies as a persistent background feature of HW events further suggests that continued Indian Ocean warming may intensify future HW risk over Sri Lanka (Rohini et al., 2016). As basin-scale warming continues under climate change, the atmospheric and thermodynamic conditions favourable for HW development are likely to become increasingly common, particularly during the FIM pre-monsoon season.

4.3. Limitations and Future Directions

This study has several limitations that should be considered when interpreting the results. First, the analysis relies primarily on ERA5 reanalysis, which provides spatially continuous and dynamically consistent atmospheric fields but has recognized limitations over complex terrain

(Zhao et al., 2023). Validation against 19 independent meteorological stations showed generally good agreement and high temporal correlations, although elevation-dependent biases were evident, with larger errors over the central highlands. These discrepancies likely reflect, in part, the 0.25° spatial resolution of ERA5, which cannot fully resolve the steep elevation gradients and associated local-scale temperature variability of Sri Lanka's mountainous interior. The percentile-based HW definition reduces the influence of systematic temperature biases, and the major HW hotspots identified in this study are predominantly located in lowland regions where ERA5 performs better. Nevertheless, some uncertainty remains in the magnitude and spatial structure of HW intensity, particularly over elevated terrain. Combining station observations with higher-resolution reanalysis or dynamically downscaled datasets would therefore improve the representation of local heat extremes in future studies.

Second, the identification of HWs using a percentile-based T_{max} threshold depends on the choice of climatological baseline (Fraser-Leonhardt et al., 2026). Because the 1995–2024 study period encompasses substantial warming over the tropical Indian Ocean, the assumption of a stationary temperature distribution may influence the estimated frequency and temporal evolution of HWs. A sensitivity analysis using an alternative 90^{th}-percentile threshold, however, produced broadly consistent spatial patterns of the major HW hotspots, indicating that the principal geographic conclusions are robust. Nevertheless, absolute event frequencies and some measures of temporal variability remain sensitive to the threshold definition. Future studies could therefore compare fixed and moving climatological baselines or apply non-stationary extreme-value approaches that explicitly account for the underlying warming trend (Thomas et al., 2023).

Third, the present analysis identifies HWs solely from T_{max}. Although T_{max} provides a robust measure of daytime thermal extremes, it does not fully represent human heat stress in a humid tropical environment, where atmospheric moisture strongly influences evaporative cooling and physiological heat strain (Khanna & Karan, 2025). The observed reduction in relative humidity during many HW events indicates a drier boundary layer, but absolute moisture levels may nevertheless remain sufficiently high to contribute substantially to thermal stress (Simath & Emmanuel, 2022). Future work should therefore complement temperature-based HW detection with integrated heat-stress metrics, including wet-bulb temperature, Heat Index, or Apparent Temperature. Such an approach would provide a more direct assessment of the implications of

humid heat for human health, occupational exposure, and labour productivity across Sri Lanka's contrasting climatic regions.

A further limitation concerns the assessment of long-term changes in HW characteristics. The 30-year record is sufficient to characterize recent HW climatology but remains relatively short for robustly separating forced trends from interannual and decadal variability associated with large-scale climate modes. This limitation is reflected in the relatively weak or statistically insignificant trends observed for some HW metrics despite their directional changes. Longer observational records, together with non-stationary extreme-value methods, would help distinguish persistent changes in HW behaviour from variability associated with natural climate fluctuations.

Finally, the composite analysis identifies a coherent sequence of atmospheric, oceanic, and land-surface anomalies associated with HWs, but the relative contribution and causality of individual processes remain to be quantified. In particular, the roles of ENSO and the Indian Ocean Dipole (IOD) in modulating the two identified seasonal HW regimes require explicit investigation. Similarly, the inferred land–atmosphere feedback could be evaluated more directly using soil moisture, evapotranspiration, and surface energy-balance observations to quantify the transition from moisture-limited to sensible-heat-dominated conditions. Future studies should also employ high-resolution regional climate simulations and multi-model projections to determine how the FIM radiative and SWM leeward HW regimes may change under continued Indian Ocean warming. Such analyses would help establish whether the spatial hotspots and seasonal mechanisms identified here are likely to persist, intensify, or shift under future climate change.

5 Summary

This study presents the first comprehensive, process-based assessment of seasonal HW variability in Sri Lanka between 1995 and 2024 and demonstrates that HW development over the island is strongly controlled by the interaction between monsoonal circulation, topography and coupled Indian Ocean–atmosphere variability. The results reveal a clear spatial concentration of HW activity over the dry-zone lowlands of northern, eastern and south-eastern Sri Lanka, where the highest frequency, intensity and persistence of events occur, while the central highlands remain comparatively less affected due to elevation-induced cooling and enhanced cloudiness. Two

seasonally distinct HW regimes were identified. The first is a pre-monsoon radiative regime during the FIM, characterized by the highest proportional contribution of HW days, elevated intensities and long event durations associated with strong solar heating, weak atmospheric ventilation and limited cloud development. The second is a leeward monsoon regime during the SWM, in which the central highlands create a pronounced rain shadow effect that maintains persistently hot conditions over the eastern and south-eastern lowlands despite active monsoon conditions elsewhere. Although SWM records the largest number of events in absolute terms due to its longer seasonal length, FIM represents the season most strongly dominated by HW conditions relative to its seasonal length.

The composite analyses further show that Sri Lankan HWs are embedded within a coherent coupled ocean–atmosphere–land process chain across the northern Indian Ocean. HW days are consistently associated with enhanced large-scale subsidence, suppressed convection, reduced cloud cover, positive OLR anomalies, and increased shortwave radiation at the surface, creating conditions favourable for radiative amplification of near-surface temperatures. These atmospheric anomalies are accompanied by rainfall deficits, reduced boundary-layer humidity, and warm Indian Ocean SST anomalies, which together reinforce atmospheric stability, surface drying, and heat persistence. The results therefore demonstrate that HWs in Sri Lanka are not simply isolated local temperature extremes, but manifestations of broader regional dynamical and thermodynamic interactions involving the tropical Indian Ocean and monsoonal circulation system. As Indian Ocean warming continues under anthropogenic climate change, the background conditions favourable for both the FIM radiative regime and the SWM leeward regime are likely to intensify, increasing the risk of more frequent, persistent, and severe HWs across Sri Lanka. These findings provide an important scientific basis for improving heat-risk assessment, seasonal early-warning capability, and climate adaptation planning in tropical island environments.

Statements & Declarations

Acknowledgement

Assistance and the facilities provided by the Department of Oceanography and Marine Geology, Faculty of Fisheries and Marine Sciences & Technology, University of Ruhuna, Sri Lanka is highly acknowledged. All open-source datasets used in this study are available from the links cited in the text. All plots and analysis are carried out using Python v.3.9 including supportive packages.

Funding

This work was supported by the University of Ruhuna Research Grant (RU/FMST/RG/2025/06) and the Southern Marine Science and Engineering Guangdong Laboratory (Zhuhai) (SML2024SP009, SML2023SP240).

Conflict of Interest statement

The authors declare that they have no conflicts of interest, financial or otherwise, related to the research, authorship, and/or publication of this article.

Author Contributions

All authors contributed to the conception and design of this study. Material preparation, data collection and analysis were performed by PG. GP contributed to the conception, design and supervision of the study. The first draft of the manuscript was written by PG and revised by GP, XG, DW, UP. All authors discussed the study results and reviewed earlier versions of the manuscript. All authors read and approved the final version of the manuscript.

Data Availability

The maximum temperature data used in this study is publicly available at https://doi.org/10.24381/cds.4991cf48 from ECMWF ERA5 reanalysis via the Copernicus Climate Data Store (CDS). To analyze the physical mechanisms of this study, the precipitation, high and low cloud cover data were obtained from the ECMWF ERA5 reanalysis via the CDS (https://doi.org/10.24381/cds.4991cf48). Atmospheric variables, including vertical velocity and surface wind component (u and v) were also obtained from the ERA5 datasets available through the CDS (https://doi.org/10.24381/cds.50314f4c). Shortwave radiation was accessed from the CDS (https://doi.org/10.24381/cds.e2161bac). Relative Humidity were obtained from the AgERA5 dataset provided by Wageningen Environmental Research via the CDS (https://doi.org/10.24381/cds.6c68c9bb). Outgoing Longwave Radiation was obtained from the NOAA Interpolated OLR dataset, provided by the NOAA Physical Sciences Laboratory (PSL), and is available at gov.noaa.ncdc:C00875. Sea Surface Temperature data is accessed through the NOAA Optimum Interpolation Sea Surface Temperature (OISST) Version 2 High Resolution dataset, also provided by NOAA PSL, and is assessable at ftp://eclipse.ncdc.noaa.gov/pub/OI-daily-v2/. Daily Surface Volumetric Soil Moisture were obtained from the C3S satellite surface soil moisture merged COMBINED product (v202505.0.0), and is assessable at https://doi.org/10.24381/cds.d7782f18

References

Abeysekera, A. B., Punyawardena, B. V. R., Marambe, B., Jayawardena, I. M. S. P., Sivananthawerl, T., & Wickramasinghe, V. N. M. (2021). Effect of Indian Ocean Dipole (IOD) Events on the Second Inter-monsoonal Rainfall in the Wet Zone of Sri Lanka. *Tropical Agricultural Research*, *32*(3), 287. https://doi.org/10.4038/tar.v32i3.8492

Alexander, L. v., Zhang, X., Peterson, T. C., Caesar, J., Gleason, B., Klein Tank, A. M. G., Haylock, M., Collins, D., Trewin, B., Rahimzadeh, F., Tagipour, A., Rupa Kumar, K., Revadekar, J., Griffiths, G., Vincent, L., Stephenson, D. B., Burn, J., Aguilar, E., Brunet, M., Taylor, M., New, M., Zhai, P., Rusticucci, M., Vazquez-Aguirre, J. L. (2006). Global observed changes in daily climate extremes of temperature and precipitation. *Journal of Geophysical Research: Atmospheres*, *111*(D5). https://doi.org/10.1029/2005JD006290

Barriopedro, D., García-Herrera, R., Ordóñez, C., Miralles, D. G., & Salcedo-Sanz, S. (2023). Heat Waves: Physical Understanding and Scientific Challenges. *Reviews of Geophysics*, *61*(2). https://doi.org/10.1029/2022RG000780

Benson, D. O., & Dirmeyer, P. A. (2021). Characterizing the Relationship between Temperature and Soil Moisture Extremes and Their Role in the Exacerbation of Heat Waves over the Contiguous United States. *Journal of Climate*, *34*(6), 2175–2187. https://doi.org/10.1175/JCLI-D-20-0440.1

Boogaard, H., Schubert, J., De Wit, A., Lazebnik, J., Hutjes, R., Van der Grijn, G. (2020). Agrometeorological indicators from 1979 to present derived from reanalysis. *Copernicus Climate Change Service (C3S) Climate Data Store (CDS)*, 1061–1079.

Cai, W., Santoso, A., Wang, G., Weller, E., Wu, L., Ashok, K., Masumoto, Y., & Yamagata, T. (2014). Increased frequency of extreme Indian Ocean Dipole events due to greenhouse warming. *Nature*, *510*(7504), 254–258. https://doi.org/10.1038/nature13327

Cai, W., Santoso, A., Wang, G., Yeh, S.-W., An, S.-I., Cobb, K. M., Collins, M., Guilyardi, E., Jin, F.-F., Kug, J.-S., Lengaigne, M., McPhaden, M. J., Takahashi, K., Timmermann, A., Vecchi, G., Watanabe, M., & Wu, L. (2015). ENSO and greenhouse warming. *Nature Climate Change*, *5*(9), 849–859. https://doi.org/10.1038/nclimate2743

Cai, W., Wang, G., Dewitte, B., Wu, L., Santoso, A., Takahashi, K., Yang, Y., Carréric, A., & McPhaden, M. J. (2018). Increased variability of eastern Pacific El Niño under greenhouse warming. *Nature*, *564*(7735), 201–206. https://doi.org/10.1038/s41586-018-0776-9

Chen, S., Ji, P., Yuan, S., Xu, Q., Lu, C., & Zhang, J. (2026). Contrary effects of soil moisture-atmosphere feedback on dry and humid heatwaves. *Nature Communications*, *17*(1), 2626. https://doi.org/10.1038/s41467-026-70210-y

Climate Change Secretariat. (2016). National adaptation plan for climate change impacts in Sri Lanka: 2016–2025. *Ministry of Mahaweli Development and Environment, Government of Sri Lanka*.

Climate Change Secretariat, M. of E. S. L. (2023). Third National Communication of Climate Change in Sri Lanka. In *Government of Sri Lanka*.

Collins, D. A., Della-Marta, P. M., Plummer, N., & Trewin, B. C. (2000). Trends in annual frequencies of extreme temperature events in Australia. *Australian Meteorological Magazine*, *49*(4), 277–292. https://doi.org/10.1071/ES00025

Cvijanovic, I., Mistry, M. N., Begg, J. D., Gasparrini, A., & Rodó, X. (2023). Importance of humidity for characterization and communication of dangerous heatwave conditions. *Npj Climate and Atmospheric Science*, *6*(1), 33. https://doi.org/10.1038/s41612-023-00346-x

Domroes, M., & Ranatunge, E. (1993). A statistical approach towards a regionalization of daily rainfall in Sri Lanka. *International Journal of Climatology*, *13*(7), 741–754. https://doi.org/10.1002/joc.3370130704

Dorigo, W., Wagner, W., Albergel, C., Albrecht, F., Balsamo, G., Brocca, L., Chung, D., Ertl, M., Forkel, M., Gruber, A., Haas, E., Hamer, P. D., Hirschi, M., Ikonen, J., de Jeu, R., Kidd, R., Lahoz, W., Liu, Y. Y., Miralles, D., Mistelbauer, Thomas., Nicolai-Shaw, Nadine., Parinussa, Robert., Pratola, Chiara., Reimer, Christoph., van der Schalie, Robin., Seneviratne, Sonia I.., Smolander, Tuomo., Lecomte, P. (2017). ESA CCI Soil Moisture for improved Earth system understanding: State-of-the art and future directions. *Remote Sensing of Environment*, *203*, 185–215. https://doi.org/10.1016/j.rse.2017.07.001

Fischer, E. M., & Schär, C. (2010). Consistent geographical patterns of changes in high-impact European heatwaves. *Nature Geoscience*, *3*(6), 398–403. https://doi.org/10.1038/ngeo866
Ford, T. W., & Schoof, J. T. (2017). Characterizing extreme and oppressive heat waves in Illinois. *Journal of Geophysical Research: Atmospheres*, *122*(2), 682–698. https://doi.org/10.1002/2016JD025721

Fraser-Leonhardt, V. A., Hegerl, G. C., & Mollard, J. D. P. (2026). Sensitivity of Heatwave Characteristics to the Climatic Baseline. *Atmospheric Science Letters*, *27*(4). https://doi.org/10.1002/asl2.70017

Hassan, W. ul, Nayak, M. A., Saharwardi, M. S., Dar, J. A., Dasari, H. P., Hoteit, I., & Abualnaja, Y. (2024). Unveiling the devastating effect of the spring 2022 mega-heatwave on the South Asian snowpack. *Communications Earth & Environment*, *5*(1), 707. https://doi.org/10.1038/s43247-024-01857-y

Hersbach, H., Bell, B., Berrisford, P., Hirahara, S., Horányi, A., Muñoz-Sabater, J., Nicolas, J., Peubey, C., Radu, R., Schepers, D., Simmons, A., Soci, C., Abdalla, S., Abellan, X., Balsamo, G., Bechtold, P., Biavati, G., Bidlot, J., Bonavita, M., De Chiara, Giovanna., Dahlgren, Per., Dee, Dick., Diamantakis, Michail., Dragani, Rossana., Flemming, Johannes., Forbes, Richard., Fuentes, Manuel., Geer, Alan., Haimberger, Leo., Healy, Sean., Hogan, Robin J., Hólm, Elías, Janisková, Marta., Keeley, Sarah., Laloyaux, Patrick., Lopez, Philippe., Lupu, Cristina., Radnoti, Gabor., de Rosnay, Patricia., Rozum, Iryna., Vamborg, Freja., Villaume, Sebastien., Thépaut, J.

(2020). The ERA5 global reanalysis. *Quarterly Journal of the Royal Meteorological Society*, *146*(730), 1999–2049. https://doi.org/10.1002/qj.3803

Horton, R. M., Mankin, J. S., Lesk, C., Coffel, E., & Raymond, C. (2016). A Review of Recent Advances in Research on Extreme Heat Events. In *Current Climate Change Reports* (Vol. 2, Issue 4, pp. 242–259). Springer. https://doi.org/10.1007/s40641-016-0042-x

Intergovernmental Panel on Climate Change (IPCC). (2023a). *Climate Change 2021 – The Physical Science Basis*. Cambridge University Press. https://doi.org/10.1017/9781009157896

Intergovernmental Panel on Climate Change (IPCC). (2023b). *Climate Change 2022 – Impacts, Adaptation and Vulnerability*. Cambridge University Press. https://doi.org/10.1017/9781009325844

Jackson, L. S., Birch, C. E., Chagnaud, G., Marsham, J. H., & Taylor, C. M. (2025). Daily rainfall variability controls humid heatwaves in the global tropics and subtropics. *Nature Communications*, *16*(1), 3461. https://doi.org/10.1038/s41467-025-58694-6

Jayawardena, I. M. S. P., Darshika, D. W. T. T., & C. Herath, H. M. R. (2018). Recent Trends in Climate Extreme Indices over Sri Lanka. *American Journal of Climate Change*, *07*(04), 586–599. https://doi.org/10.4236/ajcc.2018.74036

Karunathilaka, K. L. A. A., Dabare, H. K. v., & Nandalal, K. D. W. (2017). Changes in Rainfall in Sri Lanka during 1966 – 2015. *Engineer: Journal of the Institution of Engineers, Sri Lanka*, *50*(2), 39. https://doi.org/10.4038/engineer.v50i2.7251

Keshav, B. S., S., M. T., & Ashrit, R. (2026). Role of equatorial waves in modulating extreme temperature events over Sri Lanka. *Theoretical and Applied Climatology*, *157*(4), 242. https://doi.org/10.1007/s00704-026-06129-7

Khanna, J., & Karan. (2025). An indirect radiative surface-cooling due to water vapor in the tropics and its implications for pre-monsoonal heat stress. *Environmental Research Letters*, *20*(6), 064010. https://doi.org/10.1088/1748-9326/add174

Lee, H.-T. (2014). Outgoing Longwave Radiation - Daily - Climate Algorithm Theoretical Basis Document . *NOAA Climate Data Record Program CDRP-ATBD-0526 by CDRP Document Manager Rev.2 (2025)*, 46.

Li, Y., Zeleke, K., Wang, B., & Liu, D.-L. (2025). A Review of Data for Compound Drought and Heatwave Stress Impacts on Crops: Current Progress, Knowledge Gaps, and Future Pathways. *Plants*, *14*(14), 2158. https://doi.org/10.3390/plants14142158

Liu, J., & Pu, Z. (2019). Does Soil Moisture Have an Influence on Near-Surface Temperature? *Journal of Geophysical Research: Atmospheres*, *124*(12), 6444–6466. https://doi.org/10.1029/2018JD029750

Miralles, D. G., Teuling, A. J., van Heerwaarden, C. C., & Vilà-Guerau de Arellano, J. (2014). Mega-heatwave temperatures due to combined soil desiccation and atmospheric heat accumulation. *Nature Geoscience*, *7*(5), 345–349. https://doi.org/10.1038/ngeo2141

Miralles, D. G., van den Berg, M. J., Teuling, A. J., & de Jeu, R. A. M. (2012). Soil moisture-temperature coupling: A multiscale observational analysis. *Geophysical Research Letters*, *39*(21). https://doi.org/10.1029/2012GL053703

Pathirana, G., Oh, J.-H., Cai, W., An, S.-I., Min, S.-K., Jo, S.-Y., Shin, J., & Kug, J.-S. (2023). Increase in convective extreme El Niño events in a CO 2 removal scenario. *Science Advances*, *9*(25). https://doi.org/10.1126/sciadv.adh2412

Perkins, S. E. (2015). A review on the scientific understanding of heatwaves—Their measurement, driving mechanisms, and changes at the global scale. *Atmospheric Research*, *164–165*, 242–267. https://doi.org/10.1016/j.atmosres.2015.05.014

Perkins, S. E., & Alexander, L. v. (2013). On the Measurement of Heat Waves. *Journal of Climate*, *26*(13), 4500–4517. https://doi.org/10.1175/JCLI-D-12-00383.1

Perkins-Kirkpatrick, S. E., & Lewis, S. C. (2020). Increasing trends in regional heatwaves. *Nature Communications*, *11*(1), 3357. https://doi.org/10.1038/s41467-020-16970-7

Punyawardena, B. V. R. (2010). Climate of the Dry Zone of Sri Lanka. *Soil Science Society of Sri Lanka*, 9–26. https://doi.org/10.13140/RG.2.2.26445.15847

Punyawardena, B. V. R., & Abeysekera, A. B. (2020). The wettest place in Sri Lanka. *Sri Lanka Journal of Food and Agriculture*, *6*(2), 25–31. https://doi.org/10.4038/sljfa.v6i2.86

Renne, D., George, R., Marion, B., Heimiller, D., & Gueymard, C. (2003). *Solar Resource Assessment for Sri Lanka and Maldives*. https://doi.org/10.2172/15004299

Reynolds, R. W., Smith, T. M., Liu, C., Chelton, D. B., Casey, K. S., & Schlax, M. G. (2007). Daily High-Resolution-Blended Analyses for Sea Surface Temperature. *Journal of Climate*, *20*(22), 5473–5496. https://doi.org/10.1175/2007JCLI1824.1

Robinson, P. J. (2001). On the Definition of a Heat Wave. *Journal of Applied Meteorology*, *40*(4), 762–775. https://doi.org/10.1175/1520-0450(2001)040<0762:OTDOAH>2.0.CO;2

Rohini, P., Rajeevan, M., & Srivastava, A. K. (2016). On the Variability and Increasing Trends of Heat Waves over India. *Scientific Reports*, *6*(1), 26153. https://doi.org/10.1038/srep26153

Roxy, M. K., Ritika, K., Terray, P., & Masson, S. (2014). The Curious Case of Indian Ocean Warming. *Journal of Climate*, *27*(22), 8501–8509. https://doi.org/10.1175/JCLI-D-14-00471.1

Roxy, M. K., Ritika, K., Terray, P., Murtugudde, R., Ashok, K., & Goswami, B. N. (2015). Drying of Indian subcontinent by rapid Indian Ocean warming and a weakening land-sea thermal gradient. *Nature Communications*, *6*(1), 7423. https://doi.org/10.1038/ncomms8423

Russo, S., Sillmann, J., & Fischer, E. M. (2015). Top ten European heatwaves since 1950 and their occurrence in the coming decades. *Environmental Research Letters*, *10*(12), 124003. https://doi.org/10.1088/1748-9326/10/12/124003

Seneviratne, S. I., Adnan, M., Badi, W., Dereczynski, C., di Luca, A., Ghosh, S., Iskandar, I., Kossin, J., Lewis, S., Otto, F., Pinto, I., Satho, M., Vicente-Serrano, S., Wehner, M., Zhou, B., & Sylla, M. (2021). Weather and Climate Extreme Events in a Changing Climate. In *Climate Change 2021 – The Physical Science Basis* (pp. 1513–1766). Cambridge University Press. https://doi.org/10.1017/9781009157896.013

Seneviratne, S. I., Corti, T., Davin, E. L., Hirschi, M., Jaeger, E. B., Lehner, I., Orlowsky, B., & Teuling, A. J. (2010). Investigating soil moisture–climate interactions in a changing climate: A review. *Earth-Science Reviews*, *99*(3–4), 125–161. https://doi.org/10.1016/j.earscirev.2010.02.004

Sharma, A., Andhikaputra, G., & Wang, Y.-C. (2022). Heatwaves in South Asia: Characterization, Consequences on Human Health, and Adaptation Strategies. *Atmosphere*, *13*(5), 734. https://doi.org/10.3390/atmos13050734

Sherwood, S. C., & Huber, M. (2010). An adaptability limit to climate change due to heat stress. *Proceedings of the National Academy of Sciences*, *107*(21), 9552–9555. https://doi.org/10.1073/pnas.0913352107

Simath, S., & Emmanuel, R. (2022). Urban thermal comfort trends in Sri Lanka: the increasing overheating problem and its potential mitigation. *International Journal of Biometeorology*, *66*(9), 1865–1876. https://doi.org/10.1007/s00484-022-02328-9

SUPPIAH, R. (1996). SPATIAL AND TEMPORAL VARIATIONS IN THE RELATIONSHIPS BETWEEN THE SOUTHERN OSCILLATION PHENOMENON AND THE RAINFALL OF SRI LANKA. *International Journal of Climatology*, *16*(12), 1391–1407. https://doi.org/10.1002/(SICI)1097-0088(199612)16:12<1391::AID-JOC94>3.0.CO;2-X

Suppiah, R., & Yoshino, M. M. (1984). Rainfall variations of Sri Lanka Part 1: Spatial and temporal patterns. *Archives for Meteorology, Geophysics, and Bioclimatology Series B*, *34*(4), 329–340. https://doi.org/10.1007/BF02269446

Thomas, N. P., Marquardt Collow, A. B., Bosilovich, M. G., & Dezfuli, A. (2023). Effect of Baseline Period on Quantification of Climate Extremes Over the United States. *Geophysical Research Letters*, *50*(17). https://doi.org/10.1029/2023GL105204

Trenberth, K. E., & Fasullo, J. T. (2012). Climate extremes and climate change: The Russian heat wave and other climate extremes of 2010. *Journal of Geophysical Research: Atmospheres*, *117*(D17). https://doi.org/10.1029/2012JD018020

WHO. (2024, May 28). *Heat and Health*. World Health Organization. https://www.who.int/news-room/fact-sheets/detail/climate-change-heat-and-health

Wilks, D. S. . (2011). *Statistical methods in the atmospheric sciences* . Elsevier.

Wu, S., Luo, M., Zhao, R., Li, J., Sun, P., Liu, Z., Wang, X., Wang, P., & Zhang, H. (2023). Local mechanisms for global daytime, nighttime, and compound heatwaves. *Npj Climate and Atmospheric Science*, *6*(1), 36. https://doi.org/10.1038/s41612-023-00365-8

Xie, S.-P., Kosaka, Y., Du, Y., Hu, K., Chowdary, J. S., & Huang, G. (2016). Indo-western Pacific ocean capacitor and coherent climate anomalies in post-ENSO summer: A review. *Advances in Atmospheric Sciences*, *33*(4), 411–432. https://doi.org/10.1007/s00376-015-5192-6

Yuan, Q., Wang, G., Zhu, C., Lou, D., Hagan, D. F. T., Ma, X., & Zhan, M. (2019). Coupling of Soil Moisture and Air Temperature from Multiyear Data During 1980–2013 over China. *Atmosphere*, *11*(1), 25. https://doi.org/10.3390/atmos11010025

Zhao, P., He, Z., Ma, D., & Wang, W. (2023). Evaluation of ERA5-Land reanalysis datasets for extreme temperatures in the Qilian Mountains of China. *Frontiers in Ecology and Evolution*, *11*. https://doi.org/10.3389/fevo.2023.1135895

Zscheischler, J., Martius, O., Westra, S., Bevacqua, E., Raymond, C., Horton, R. M., van den Hurk, B., AghaKouchak, A., Jézéquel, A., Mahecha, M. D., Maraun, D., Ramos, A. M., Ridder, N. N., Thiery, W., & Vignotto, E. (2020). A typology of compound weather and climate events. *Nature Reviews Earth & Environment*, *1*(7), 333–347. https://doi.org/10.1038/s43017-020-0060-z

Zubair, L., Siriwardhana, M., Chandimala, J., & Yahiya, Z. (2008). Predictability of Sri Lankan rainfall based on ENSO. *International Journal of Climatology*, *28*(1), 91–101. https://doi.org/10.1002/joc.1514

Supplementary Files

This is a list of supplementary files associated with this preprint. Click to download.

- SLHWSupplementarymaterial.docx